T.R.
BOLU ABANT İZZET BAYSAL UNIVERSITY
INSTITUTE OF GRADUATE STUDIES
Department of Chemical Engineering

DESIGN AND UTILIZATION OF A NOVEL TRICKLE-BED ELECTROCHEMICAL REACTOR FOR ADVANCED TREATMENT OF SYNTHETIC WASTEWATER

MASTER OF SCIENCE

FKRAT ALI TAQI

ACADEMIC SUPERVISOR
Assoc. Prof. Dr. Musa BÜYÜKADA
ACADEMIC CO-SUPERVIZOR
Assist. Prof. Dr. Ghassan H. Abdullah

BOLU, JUNE - 2024

APPROVAL OF THE THESIS

Design and utilization of a novel trickle-bed electrochemical reactor for advanced treatment of synthetic wastewater submitted by **Fkrat Ali Taqi** and defended before the Examining Committee Members listed below in partial fulfillment of the requirements for the degree of **Master of Science** in**, Chemical Engineering, Institute of Graduate Studies of Bolu Abant Izzet Baysal University on 27.06.2024** by

Examining Committee Members	**Signature**
Supervisor Assoc. Prof. Dr. Musa BÜYÜKADA Bolu Abant İzzet Baysal University	.....
Member Prof. Dr. Muhammet Yıldırım Bolu Abant İzzet Baysal University	.....
Member Assist. Prof. Dr. Emine EKİNCİ Gazi University	.....

Prof. Dr. İbrahim KÜRTÜL

Director of Instıtute of Graduate Studies

ETHICAL DECLARATION

In this thesis dissertation that was properly prepared according to the Thesis Writing Rules of Bolu Abant İzzet Baysal University of the Institute of Graduates Studies, I hereby declare that;

- All data, information, and documents presented in the thesis were obtained in accordance with the academic and ethical rules,
- All data, documents, assessments, and results were presented in accordance with the scientific ethical and moral rules,
- All works that were benefitted in the thesis were appropriately cited,
- No alteration was made in the data used,
- Study presented in this thesis is original,

Otherwise, I declare that I accept the loss of all my rights in case any contradiction that may arise against me.

The similarity rate obtained by using the Turnitin program, a plagiarism detection software, is within the limits approved by the University Senate.

Fkrat Ali Taqi

ABSTRACT

DESIGN AND UTILIZATION OF A NOVEL TRICKLE-BED ELECTROCHEMICAL REACTOR FOR ADVANCED TREATMENT OF SYNTHETIC WASTEWATER
MSC THESIS
FKRAT ALİ TAQI
BOLU ABANT İZZET BAYSAL UNIVERSITY
INSTITUTE OF GRADUATE STUDIES
DEPARTMENT OF CHEMICAL ENGINEERING
SUPERVISOR: ASSOC. PROF. DR. MUSA BÜYÜKADA
CO-SUPERVISOR: ASSIST. PROF. DR. GHASSAN H. ABDULLAH
BOLU, JUNE 2024
(xiv + 71)

In the present thesis, the design and utilization of an innovative and novel trickle bed electrochemical reactor for the advanced treatment of synthetic wastewater was aimed. In this reactor, firstly, the reduction of dissolved oxygen on the surface of a cathode composed of carbon and polytetrafluoroethylene (C-PTFE) was carried out, followed by electrochemical production of hydrogen peroxide (H_2O_2). Subsequently, catalytic decomposition-based generation of hydroxyl radicals was carried out. These hydroxyl radicals were used to oxidize the methyl orange (MO) as an organic pollutant. The cathode design in the TBER was obtained from a double-layer bed consisting of a C-PTFE mixture tightly attached to a stainless-steel mesh. Thus, both a highly efficient electrode and a continuously operating treatment process were aimed. The effectiveness of different operating parameters such as voltage, initial MO concentration, oxygen flow rate, electrolyte flow rate, KOH concentration and temperature were investigated to increase the removal efficiency. The optimum operating conditions were determined as 1 V, 20 ppm, 7 L/min oxygen flow rate, 200 mL/min electrolyte flow rate, 0.2 M KOH concentration and 30^{o}C. Maximum MO removal of 98% was achieved under these conditions. Kinetic studies showed that the MO degradation process fitted well with pseudo-first order kinetics. The reaction rate constant was calculated as 0.0179 1/min at 30°C and 0.0111 1/min at 5°C. Based on these calculations, the activation energy of the TBER-based MO removal process was obtained as 14.062 kJ/mol. Thermodynamic studies showed that the TBER was endothermic and spontaneously. As a result, the experimental findings were found to be in great accordance with the related literature and TBER was considered to be a promising process.

KEYWORDS: Methyl orange, Trickle bed reactor, Wastewater treatment, Kinetic, Thermodynamic.

ÖZET

SENTETİK ATIK SULARIN İLERİ ARITILMASI İÇİN YENİ BİR DAMLAMA YATAKLI ELEKTROKİMYASAL REAKTÖRÜN TASARIMI VE KULLANIMI
YÜKSEK LİSANS TEZİ
FKRAT ALİ TAQI
BOLU ABANT İZZET BAYSAL ÜNİVERSİTESİ
LİSANSÜSTÜ EĞİTİM ENSTİTÜSÜ
KİMYA MÜHENDİSLİĞİ BÖLÜMÜ

TEZ DANIŞMANI: DOÇ. DR. MUSA BÜYÜKADA
İKİNCİ DANIŞMAN: DR. ÖĞR. ÜYESİ GHASSAN H. ABDULLAH
BOLU, HAZİRAN - 2024
(xiv + 71)

Mevcut tez çalışmasında, sentetik atıksuların ileri arıtımı için yenilikçi ve sıra dışı bir damlama yataklı elektrokimyasal reaktörün tasarımı ve kullanımı hedeflenmiştir. Bu reaktörde, önce karbon ve politetrafloroetilenden (C-PTFE) oluşan bir katodun yüzeyinde çözünmüş oksijenin indirgenmesi, sonrasında ise elektrokimyasal olarak hidrojen peroksit (H_2O_2) üretimi gerçekleştirilmiştir. Devamında, katalitik ayrışma-temelli hidroksil radikallerinin üretimi gerçekleştirilmiştir. Bu hidroksil radikalleri metil turuncu organik kirleticisini oksitlemek için kullanılmıştır. TBER'deki katot tasarımı, paslanmaz çelik bir ağa sıkı bir şekilde tutturulmuş C-PTFE karışımından oluşan çift katmanlı bir yataktan elde edilmiştir. Böylelikle hem etkinliği yüksek bir elektrot elde etme hem de sürekli çalışan bir arıtma süreci hedeflenmiştir. Giderim verimini artırmak için voltaj, başlangıç MO konsantrasyonu, oksijen akış hızı, elektrolit akış hızı, KOH derişimi ve sıcaklık gibi farklı işletme parametrelerinin etkinlikleri incelenmiştir. Optimum çalışma koşulları 1 V, 20 ppm, 7 L/dk oksijen akış hızı, 200 mL/dk elektrolit akış hızı, 0.2 M KOH derişimi ve 30^{o}C olarak belirlenmiştir. Bu şartlarda maksimum MO giderimi olan %98 sonucuna ulaşılmıştır. Kinetik çalışmalar, MO bozunma sürecinin sözde birinci derece kinetiğe uydun olduğunu göstermiştir. Reaksiyon hız sabiti 30°C'de 0,0179 1/dk, 5°C'de ise 0,0111 1/dk olarak hesaplanmıştır. Bu hesaplamalara istinaden TBER-temelli MO giderim sürecinin aktivasyon enerjisi 14,062 kJ/mol olarak elde edilmiştir. Termodinamik çalışmalar TBER'in endotermik ve kendiliğinden olduğunu göstermiştir. Sonuç olarak, elde edilen deneysel bulguların ilgili literatür ile büyük bir uyum içerisinde olduğu görülmüş ve TBER'in gelecek vaad eden bir süreç olduğu değerlendirilmiştir.

ANAHTAR KELİMELER: Metil turuncu, Damlama yataklı reaktör, Atık su arıtımı, Kinetik, Termodinamik.

TABLE OF CONTENTS

Page

LIST OF FIGURES

Page

LIST OF TABLES

Page

LIST OF ABBREVIATIONS AND SYMBOLS

AOPs : Advanced oxidation procesess

ACF : Activated carbon fiber

AO7 : Acide orange 7

AO : Anode oxidation

AC : Activated carbon

BCD : Biochemical oxygen demand

BDD : Boron-doped diamond

BB3 : Basic Blue 3

CB-PTFE : Carbon black-Polytetrafluoroethylene

COD : Chemical oxygen demand

DS : Dissolved solids

DTNA : Self-doped TiO_2 nanotube array

3DER : three-dimensional electrode reactor

2DER : two-dimensional electrode reactor

EOPs : Electrochemical advanced oxidation processes

EF : Electro-Fenton

EO : Electrochemical oxidation

EG : Exfoliated graphite

E_a : Activation energy

E_R : Average energy

E_{TS} : Average thermo-dynamical energy

FTIR : Fourier-transform infrared spectroscopy

GDEs : Gas diffusion electrodes

GAC : Graunlar activated carbon

HfMBR : Hollow fiber membrane bioreactor

HRT : Hydraulic retention time

HPLC : High Performance Liquid Chromatography

ICBR : internal circulation batch reactor

LC-MS : Liquid chromatography mass spectrometry

MO : Methyl orange

MG : methyl green

MB : Methylene blue

MMO : Mixed metal oxides

MGDE : Modified gas diffusion electrode

MWCNT : Multiwalled carbon nanotubes

NHE : normal hydrogen electrode

OMMT : Organically modified Ca-montmorillonite

ORR : Oxygen reduction reaction

PSA : Porous starch aerogel

PTFE : Polytetrafluoroethylene

PE : Photoelectro-Fenton

ROS : Reactive oxygen species

RVC : Reticulated vitreous carbon

RSAC : Reed straw activated carbon

RR195 : Reactive Red 195

rGO : Reduced graphene oxide

SS : Suspended solids

SPS-fabricte : Spark plasma sintering

SE : Sono-Electrochemistry

SEBR : Square-shaped electrolytic batch reactor

TSSA-ADC : Ti/SnO_2-Sb anode – air dif- diffusion cathode

TBER : Trickle Bed Electrochemical Rector

TOC : Total organic carbon

WAO : Wet air oxidation

ACKNOWLEDGEMENTS

Sincere thanks to ALLAH, for the wisdom, strength, peace of mind and good health he has given me to finish this research.

Firstly, the author wishes to express his deepest gratitude to his supervisor Assoc. Prof. Dr. Musa BÜYÜKADA for enlightening my road, his guidance, advice, criticism, encouragements, and insight throughout the research.

Subsequently, the author would like to present his special thanks to Assist. Prof. Dr. Ghassan H. Abdullah, co-supervisor, for his assistance in lab-scale studies and supplying the facilities.

Additionally, the author would also like to thank to Assist. Prof. Dr. Mohammed Mizhar for his suggestions and comments.

This thesis study was performed by the support of the Department of Chemical Engineering, Tikrit University, Iraq. So, the author would like to clearly express his sincere appreciation to labrotary staff for support in providing the research facilities. Additionally, all the experiments, analysis and data production were performed at Tikrit University with the aid of one of ongoing projects of Dr. Ghassan. Therefore, the author would like to clearly state that he takes all the responsibility of performing the experiments and producing data.

Finally, the author would like to present his inner thanks to Hareth Abbas Faraj due to his help, motivation, and encouragement.

1. INTRODUCTION

Although the earth is known as the water planet because it contains 75% water, this water is unsuitable for domestic purposes. Ocean water is naturally salty and unfit for human consumption. Freshwater accounts for around 2.7 percent of the total water on the planet (1). Table 1.1 depicts the fraction of water present on earth from different sources. The world's growing population and industrial lifestyle have intensified anthropogenic effect on the environment. Thus, urbanization and industrialization have dramatically increased wastewater production (2). Since water is fundamental to human survival, there is an ever-increasing demand to ensure that it remains of high quality. There are a variety of environmental and global changes, including industrial, agricultural, and household run off, that are the main culprits behind water contamination. In many parts of the globe, both underground and surface water are contaminated and useless for human consumption.

Table 1.1 Relative proportion of water in different sources (1)

Source	Relative proportion (%)
Water in oceans	97.39
Water in the river and lakes	0.02
Water present in the atmosphere as vapors	0.001
Water in glaciers and polar ice caps etc.	2.01
Underground water and soil moisture	0.58
Total hydrosphere fresh water	2.6

One of the most critical problems facing the world today is the rise in organic compound contamination of water supplies caused by a wide range of human activities in the agricultural, industrial, and urban sectors. It has been clearly stated as quite difficult to break organic compounds down using conventional methods. These compounds are generally defined as persistent organic pollutants which lead to the formation of bulk. Consequently, they have been discovered in water sources all around the world, including potable water, rivers, lakes, and seas. Because they are poisonous and have harmful impacts on human health and the environment, efficient removal of organic compounds has

been on demand (2,3). Before discharge into the environment and water reuse, and for dealing with the growing release of harmful and nonbiodegradable pollutants (4).

Efficient removal of those organic pollutants needs a certain vast amount of water. This vast amount of wastewater is needed to be treated efficiently, given the complex structure of the organic pollutants. A further understandable way may be foreseen when the specific activity-based water usages are shared depending on the industries such as irrigation, industrial, and domestic purposes (Table 1.2). Table 1.2 demonstrates the water consumption in Turkey between 2012 and 2023by sectors. The significant increase in water consumption from 50 to 112 billion m^3 points out the importance of the issue (5) .

Table 1.2 Water Consumption by Sectors in Türkiye (5).

Water Consumption/Year	2012 ($10^9\ m^3$)	2023 ($10^9\ m^3$)
Industrial	7	22
Domestic	7	18
Irrigation	36	72
Total	50	112

The primary pollution that harms living things is water pollution from manufactured dyes, which is also an important issue because dyestuffs are made worldwide. Multiple studies have shown that there are over 100,000 different dyes on the market and that more than 7×10^5 tons of dyestuffs are made every year (6). Manufacturing processes use about 200 to 350 m^3 of water per ton of made products in sectors like textiles, cosmetics, paper, leather, and agricultural research (7). It is also important to note that the amount of leftover waste increases in a very interesting way as a country becomes more industrialized. There are currently nearly five million identified chemicals registered, of which about 70,000 are frequently utilized around the world. Every year, about 1,000 new compounds are added to the list (8). Several Asian countries depend on the textile industry for their economies. India consumes around 80% of dyestuffs and is the second-largest exporter of dyes after PRC, where nearly 1.5×10^5 tons of effluent are being discharged to the environment (7). In related literature, particularly three ways have come forward as one of the major approaches to treat polluted industrial water as physical, chemical, and, biological methods. Table 1.3

shows typical properties of textile sector effluent, which vary significantly from sample to sample.

Table 1.3 Composite Textile Industry Wastewater Characteristics (9).

Parameter	Range
pH	7.0 - 9.0
Biological oxygen demand (mg/L O_2)	80 - 6000
Chemical oxygen demand (mg/L O_2)	150 -12000
Total suspended solid (mg/L)	15 - 8000
Total dissolved solid (mg/L)	2900 - 3100
Chloride (mg/L)	1000 - 1600
Total Kjeldahl Nitrogen (mg/L)	70 - 80

The textile industry consumes more than 70% of all dyes produced globally (7,10). The discovery of dye in effluent, even in small amounts (less than 1 mg/dm3 for few days), is a significant concern and inappropriate (10). As a result, 2.2 million people die each year due to water poverty, which is a terrible outcome. (11), many of them children. For this reason, water from textile industries must be treated before being discharged into the environment. Textile processing is one of the most popular sectors globally, and depending on the characteristics of the raw material and finished product, it utilizes a wide range of chemicals. Some of these substances include enzymes, detergents, dyes, acids, sodas, and salts. Discharge of wastewater with high concentrations of reactive dyes is a well-known issue connected with dyestuff activities (8). Because these chemicals are found in industrial wastewater and textile wastewater release, we need to find alternatives to the well-known traditional methods treatment in order to get rid of the remaining water effectively (8). There are a variety of technologies that can be used in this context, including physical processes like sorption, membrane, and filtration; chemical methods like coagulation and enhanced oxidation; and biological approaches like aerobic and anaerobic microbial degradation and the use of pure enzymes (7).

These methods have been found to be ineffective in treating dye. Thus, it is necessary to develop modern technologies for their processing. Among these technologies, electrochemical processing technology has gained high attention from researchers.

1.1 Conventional strategies to remove dyes

1- Biological processes: Biological remedies are the most extensively utilized category of wastewater remediation methods due to their economical nature. However, they are incapable of treating toxic and non-biodegradable substances (12), and their long treatment periods (up to several months), expansive implementation areas, and sensitivity to environmental conditions (microorganisms) can cause operational complications.

2- Physical processes: Physical processes separate contaminants from water. The fundamental issue with these approaches is their inability to break down organic contaminants, thus leading to their transfer from liquid to solid phases and the need for extra solid phase treatment. It can cost a lot to use adsorption and separation of membranes due to the need for them to be cleaned up and thrown away from residues (13).

3- Chemical processes: To eliminate pollutants or change their structure, traditional chemical processes typically employ oxidative agents. Hydrogen peroxide (H_2O_2) and chlorine dioxide (ClO_2) are both well-known oxidatives; nevertheless, the use of chlorine species might result in the formation of organochlorinated intermediates, which have the potential to cause cancer (14). As an important application way for chemical treatment, advanced oxidation processes (AOPs) based on the theory of which formation of independent hydroxyl radicals ($OH^{\bullet}$) in the media. These radicals react with organic compounds and can lead to a degradation of them (15).

Treatment approaches for dye removal from different industrial wastes can be mainly split into three types, as observed in Figure 1.1. Additionally, these techniques are further subdivided into several elimination methodologies.

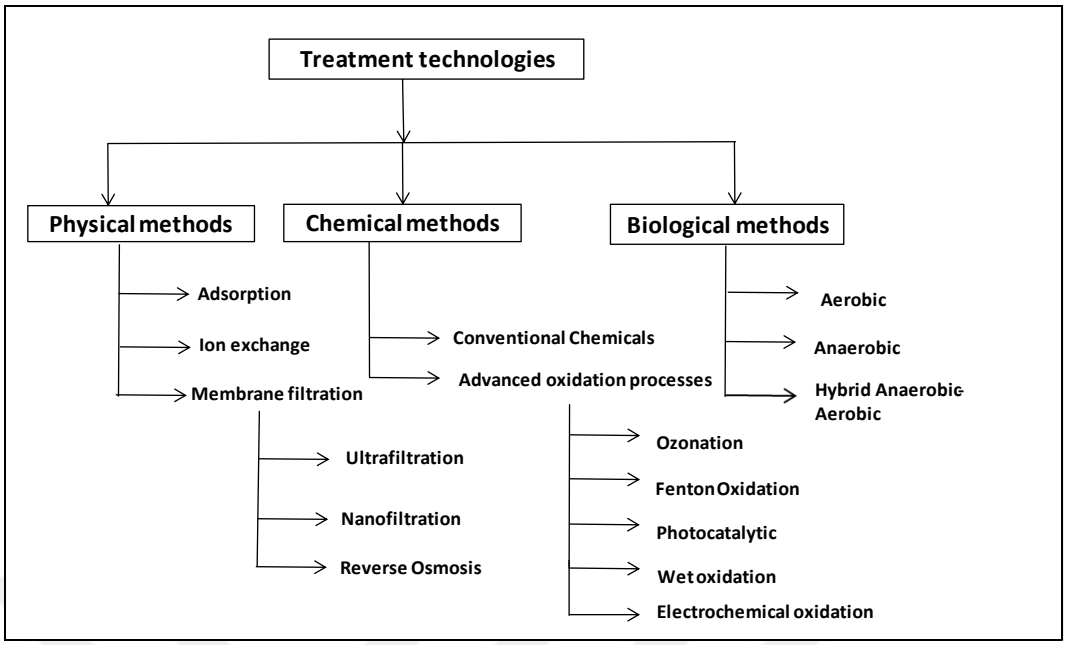

Figure 1.1 Various treatment technologies for the degradation of methyl orange from textile wastewater.

By advanced oxidation processes, we mean a suite of innovative, environmentally friendly techniques for enhancing the effectiveness of present wastewater treatment systems and reducing the impact of pollutants. Due to the high efficiency and rapid reaction rate (16), and especially the absence of very dangerous residuals. Advanced oxidation techniques utilize in situ-produced hydroxyl radicals $OH^{\bullet}$, a more reactive molecule than chlorine and hydrogen peroxide (17), $OH^{\bullet}$ can be created in a variety of ways, and AOPs are categoriezed based on the mechanism included in the radical formation, which can be chemical, photochemical, electrochemical, or sonochemical (12).

In the 1980s, for the treatment of potable water, advanced oxidation processes (AOPs) employing potent hydroxyl or sulphate radicals as the principal oxidizing agent were first proposed (18). Subsequently, AOPs were extensively utilized in the treatment of various types of wastewater due to the fact that the potent oxidants degraded resistant organic pollutants and inorganic pollutants in wastewater. All advanced oxidation processes start with the generation of hydroxyl radicals ($OH^{\bullet}$) in situ. Hydroxide radical ($OH^{\bullet}$) is the second most reactive species after the fluorine atom, and it starts a chain reaction of oxidation reactions that result in mineralization products for instance carbon dioxide (CO_2), water (H_2O), and mineral acids (HCl, HNO_3, H_2SO_4, etc.) for any Cl, N, S, etc. In

the pollutants and their byproducts (16). $OH^{\bullet}$ may attack organic compounds in three ways, which include the following: dehydrogenation or removal of a hydrogen atom to generate water, hydroxylation or electrophilic addition to a nonsaturated bond, and electron transfer or redox reactions (18).

Advanced oxidation processes (AOPs) are currently offered as an effective and growing approach for treating effluent that carries harmful or recalcitrant organic contaminants. Several methods exist, including UV-hydrogen peroxide, Fenton and photo-Fenton oxidation, and ozone-based reactions. Photocatalysis, sonolysis, electrochemical oxidation, and their combination mechanisms have all been studied (15). Among these AOPs, electrochemical advanced oxidation processes (EAOPs), which were created in the last ten years, have gotten a lot of attention as a way to get rid of persistent organic pollution like synthetic dyes. EAOPs break down organic pollution by using hydroxyl radicals that are made electrolytically. EAOPs can be divided into two kinds: direct oxidation at the anode and indirect oxidation at the cathode (19,20). The electrode material chosen plays an important role in oxidation processes. Electrochemical Advanced Oxidation Processes (EAOPs) have developed as environmentally benign technologies with great potential. Among the several advantages of these electrochemical treatment techniques are as follows:

i. The approaches do not require the external addition of any chemicals to the system to generate hydroxyl radicals.
ii. Using electrons as a cleaning reagent in a process.
iii. The operations are carried out at room pressure and temperature.

1.2 Classification of Dyes

Dyes are organic substances that give color to various things like plastics, textiles, cosmetics, waxes, paper, and pharmaceuticals when incorporated into them (21). Dyes are categorized as azo dyes and anthraquinone dyes according to the chemical structure of the chromophore group (22).

1. Anthraquinone dyes: Anthraquinone dyes are the second most popular type of textile dye, after only azo dyes, in terms of their usage. Even though that these dyes have a wide variety of colors that span almost the

whole visible spectrum, the most common applications for them are in the production of violet, blue, and green hues (23).

2. Azo dyes: Azo-dyes are extremely hazardous and carcinogenic as a result of their degradation into amines. The yearly global production of azo dyes is expected to be one million tonnes, and there are currently over 2,000 chemically different azo dyes in use (24). The main type of synthetic dyes used in many commercial applications are aromatic compounds that include one or more -N=N- groups, making up around 60–70% of all dyestuffs produced. Azo dyes can have different numbers of azo linkages: mono-azo dyes have one connection, diazo dyes have two, and triazo dyes have three. The presence of one or more azo groups (R1-N=N-R2) connected to aromatic rings typically substituted by sulfonate groups defines azo dyes. Aromatic replacement compounds with a conjugated system are responsible for the intense color, enhanced solubility in water, and resistance to degradation of azo dyes in natural environments (23).
3. Indigoid dyes: Also known as 2,2′-bis-indole, is one of the oldest dyes known. It's also one of the most widespread; it makes up 3% of all dyes made. The primary application commercial enterprises utilize it for is to color blue jeans and other blue denim items (25). Its poor solubility and very high melting point (390–392°C) are both explained by the strong intermolecular hydrogen bonds that it has. Indigo molecules are linked to four molecules in the area around them. Nonpolar liquids most commonly contain indigo as a monomer (25).
4. Triarylmethane dyes: Dyes are widely employed in the textiles sector to dye wool, nylon, cotton, and silk, as well as waxes, plastics, and oils. The phototoxicity of triarylmethane dyes, which is determined by their ability to produce reactive oxygen species, has been extensively researched to evaluate their potential for photodynamic therapy. However, their photostability remains relatively low (26).

1.3 Methyl Orange

Methyl orange, or (MO) dimethylaminoazobenzenesulfonate, is a popular and typical azo anionic dye. This manufactured organic dye that dissolves in water has a very high level of colorability and turns a bright orange color when

mixed with water. Azo dyes, for instance methyl orange, consist of aromatic compounds with the presence of -N=N- groups within their molecular structures (27), as shown in Figure 1.2. These compounds are known to possess high toxicity, carcinogenicity, and teratogenicity. They pose a significant threat to life, organisms, and the environment (28). According to the weight of the molecular structure, the molecular diameter is estimated to be between 6 and 8 nm.

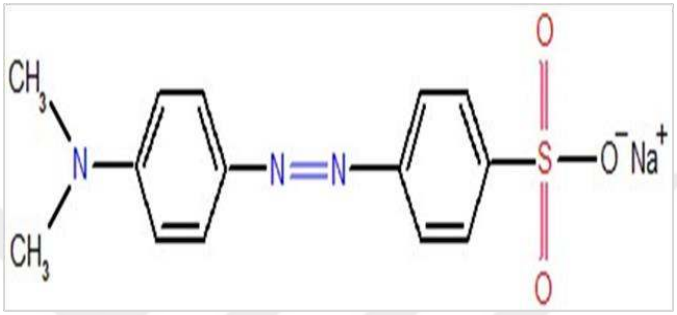

Figure 1.2 Schematic diagram of molecular structural formula of methyl orange (29).

2. LITERATURE SURVEY

2.1 Synthetic dyes

Mani et al., 2019 stated that synthetic dyes are being used more commonly in a variety of industries like textiles, leather, pharmaceuticals, food, and etc (13). Lin et al., 2016 reported that at least 10,000 dyes were considered as available for commercial use and were developed and utilized in the manufacturing sector by the end of the 19th century (10,30). Brillas et al., 2015 pointed out that in every year, 280,000 tons of dyes are being dumped into the environment around the world (31). Hussain et al., 2020 investigate that the textile industry is responsible for the consumption of about 50–70% of total manufactured dyes worldwide (10). 1-2% of dyes are lost through production, and 10-15% are discharged as effluent during dye applications (10). Vijayaraghavan et al.,2013 illustrated that in the textile industry, 200 to 500 liters of water are required for each kg of finished product (32).

Brillas et al., 2009 demonstrated that dyes can be categorized into many types such as acidic, basic, direct, sulfur, reactive, disperse, and metal complexes. Lin et al., 2016 showed that more than 70% of all dyestuffs used globally are azo dyes, which are defined by one or two azo bonds (-N=N-) (30). Whenever these dye-contaminated waters are disposed of improperly, they will contaminate a wider variety of environmental matrixes, including surfaces, ground, drinking water, and soils. Because of chemical stability and biological resilience, this is an unfortunate reality, as described by Pereira et al., 2012 (7). In most cases, azo dyes are not suitable for treatment by conventional wastewater technologies (33). For this reason, many studies have primarily focused on removing azo dyes from water (34).

2.2 Electrochemical oxidation processes

The electrochemical procedure consists of the oxidation and conversion or degradation of organic molecules into a non-toxic and harmless product using an electric current (35,36). The technique can be quite cost-effective because it only needs a small quantity of chemicals, and it's easy to keep the process stable by changing the voltage of the electricity (37). Prominent electrochemical oxidation processes (EAOPs) encompass anodic oxidation (AO) (35), which yields

heterogeneous $OH^{\bullet}$ at the anode surface, besides, electro-Fenton (EF) (14,38,39), photoelectro-Fenton (PEF) (31,40), and sono-electrochemistry (SE) (19), which produce homogeneous $OH^{\bullet}$ in bulk solution, respectively. Additionally, diverse EAOPs, including AO, can be coupled with EF, PEF, or SE to generate $OH^{\bullet}$ that are both heterogeneous and homogeneous. They frequently occur concurrently.

In both situations, the electrochemical cell is subjected to high cell voltages in order to sustain the anode activity while simultaneously oxidizing water and contaminants. Low cell voltages are often used to stop O_2 evolution, but this can cause the anode to lose its activity because some byproducts of direct anodic oxidation can stick to the anode's surface (40). Dye can be broken down electrochemically in two different ways: either directly on the anodic electrode of the cell or indirectly via reactive oxygen species (ROS) that occur on the anode surface when water oxidises. Both of these methods are possible. Furthermore, combining physical and chemical methods with electrochemical processes is highly beneficial, with reactive electrochemical membranes serving as an ideal example.

2.2.1 Anode oxidation

2.2.1.1 Direct anode oxidation

Brillas et al.,2015 reported that anodic oxidation, or EO, is the most widely used electrochemical approach for eliminating organic waste from wastewater. It is one of the electrochemical advanced oxidation processes (EAOPs) (31). Huitle et al., 2015 indicated that the beginning, with early research by Dabrowski in the 1970s, subsequent investigations by Kirk, Stucki, Kotz, Chettiar, and Watkinson in the 1980s, and the work of Johnson, Battisti and Comninellis in the 1990s, provided a fundamental understanding of EO in relation to its potential as an alternate technique for treating wastewater (41). During oxidation, contaminants are initially adsorbed on the electrode's surface without the presence of any further components besides electrons. These substances are frequently referred to as pure reagents. In theory, it is possible to achieve direct electro-oxidation at lower potential ranges prior to oxygen evolution. Nevertheless, this process is frequently characterized by slower kinetics and is dependent on the electro-catalytic ability of the anode.

Jasim., 2023 reported the employing of noble metals, such as Pd or Pt, as well as the implementation of anodes composed of metal oxides like PbO_2, IrO_2, TiO_2-Ru, and Ir-TiO_2, has been observed to enhance the rate of electrochemical processes (42). The direct Anode Oxidation (AO) process can be described as a form of electrochemical advanced oxidation processes (EAOPs), where in the breakdown of organic pollutants mostly takes place through the action of hydroxyl radicals that are adsorbed onto high O_2 overvoltage anodes during water oxidation. The breakdown pathway of organic pollutants in the (AO). The approach is displayed in Figure. 2.1.

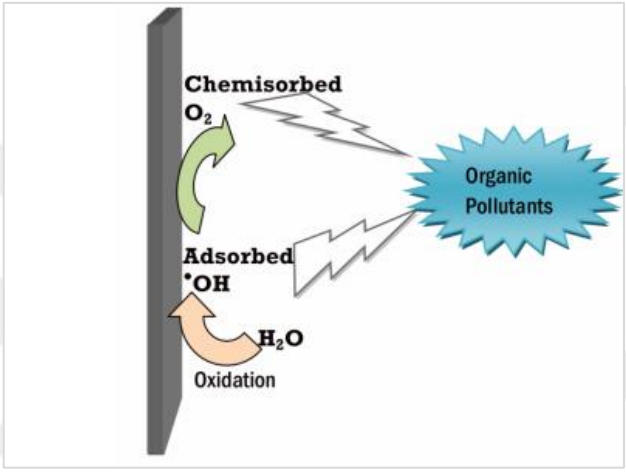

Figure 2.1 Mechanism of free radical formation reaction and elimination organic pollutant in AO process(19).

Oxidation of water is the primary source of the heterogeneous hydroxyl radical MO_x ($OH^{\bullet}$), according to Eq. 2.1. It can be seen in Eqs. 2.2 and 2.3 that the adsorbed radicals produce both chemisorbed oxygen and oxygen evolution. The chemisorbed oxygen also undergoes a process that results in oxygen, as shown in Eq. 2.4 (19).

$$MO_X + H_2O \rightarrow MO_X(HO^{\bullet}) + H^+ + e^- \qquad 2.1$$

$$MO_X(HO^{\bullet}) \rightarrow MO_{X+1} + H^+ + e^- \qquad 2.2$$

$$MO_X(HO^{\bullet}) \rightarrow MO_X + H^+ + e^- + 0.5\,O_2 \qquad 2.3$$

$$MO_{X+1} \rightarrow MO_X + 0.5\,O_2 \qquad 2.4$$

As shown in Eqs. 2.5 and 2.6, the MOx ($OH^{\bullet}$) and oxygen oxidize the organic pollutant. And then catalytic regeneration of the anode surface is described by Eqs. 2.3–2.6.

$$MO_X(HO^{\bullet}) + RH \rightarrow MO_X + H_2O + R^{\bullet} \qquad 2.5$$

$$MO_{X+1} + RH \rightarrow MOx + RHO \qquad 2.6$$

Nidheesh and Zhou, 2018 found that the oxidants generated in the AO electrolytic cell, MO_x ($OH^{\bullet}$), lead organic contaminants to fully mineralize, while chemisorbed oxygen ($MO_x(OH^{\bullet})$) results in the organic contaminants selectively oxidizing (19). A number of researchers have looked into the AO process as a means of removing dye from aqueous solutions. Faouzi et al, 2007 reported that the anode oxidation process using a BDD anode could mineralize and completely break down alizarin red S. They got a high removal efficiency at both low and high current densities (43). Zhao et al, 2009 reported that methyl orange was completely broken down in the presence of a platinum electrode activated by microwaves. The investigations were conducted within a circulating system operating at atmospheric pressure (44).

2.2.1.2 Indirect anode oxidation

In indirect electrochemical oxidation, electrolysis creates a potent oxidizing agent at the anode surface. This oxidizing agent then gets rid of the contaminants in the bulk solution. This oxidizing agent operates as an intermediary in the process of electron transport from the electrode to the organic component. There are a variety of electrochemical oxidation methods to eliminate the pollutants. Jasim et al., 2023 concluded that anodically produced chlorine and hypochlorite can effectively eliminate pollutants. Figure 2.2 shows a simplified diagram of the two mechanisms: direct and indirect.

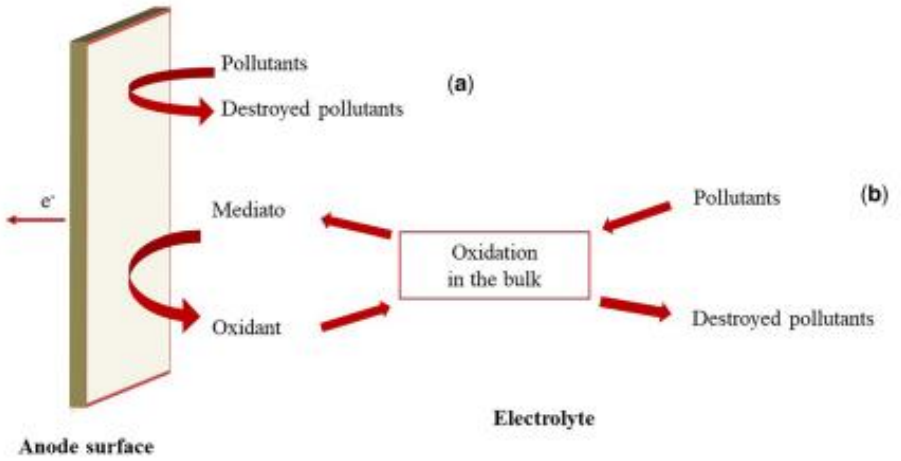

Figure 2.2 The diagrams depict (a) direct and (b) indirect pollutant oxidation processes (45).

Indirect electrical oxidation is utilized for purifying water that has been polluted with organic contaminants. This process involves the interaction of the pollutants with active chlorine species, including Cl_2, HClO, or ClO, present in the mixture (46). The steps outlined in the equations below can create these types of species at the anode surface of a Boron-Doped Diamond (BDD) electrode (47).

$$2Cl^- \rightarrow Cl_2 + 2e^- \qquad 2.7$$

$$Cl^- + 2OH^- \rightarrow ClO^- + H_2O + 2e^- \qquad 2.8$$

$$Cl_2 + H_2O \rightarrow HClO + H^+ + Cl^- \qquad 2.9$$

$$HClO \rightarrow H^+ + ClO^- \qquad 2.10$$

Sodium chloride, a salt compound, was introduced into the wastewater to enhance conductivity and facilitate particular electrochemical processes at the surface of the electrodes (47). Anantha and Venkatesha, 2014 looked at the breakdown of MG, MO, and MB in both undivided and divided cell systems using various electrode components. Metals such as Al and Zn outperformed Cu and Pt. Changes in the pH of the wastewater matrix affected the elimination of color and COD. The increased acidic pH in the separated cell accelerated the elimination of color and COD (48). Santos et al., 2014 are reported that recent studies commonly utilize titanium as a foundation to sustain Sb-SnO_2 coatings. Nevertheless, the simplest form of Ti/Sb-SnO_2 is inappropriate for applications in industry because of its poor stability and limited electrochemical oxidation kinetics (49). Lazhar et

al., 2017 showed that the performance of PbO_2 and $TiRuSnO_2$ anodes in oxidizing a synthetic solution containing IC. Showed that in the presence of 825 ppm of NaCl, the $TiRuSnO_2$ anode was more efficient than PbO_2 (50). Wang et al., 2019 reported that SPS-fabricated Ti_4O_7 bulks with good electrical conductivity were employed as MO electrochemical oxidation electrodes. MO was almost fully removed after 2 hours under all experimental circumstances, with COD reaching 91.7% elimination under 10 mA/cm and 100 mg/L initial MO concentration after 5 hours of electrolysis. Ti_4O_7 electrodes performed better than commercial electrodes in electrochemical oxidation (51).

These approaches may improve the electrochemical oxidation (EO) performance of the electrodes and increase the lifespan of the electrodes to some extent. Nevertheless, the presence of technological challenges and exorbitant expenses renders their implementation in actual scenarios arduous. Hence, it remains a difficult task to discover a straightforward and cost-effective method for producing superior Sb-SnO_2 electrodes (52). This type of process uses up some of the cell's current and makes the current less efficient. Experts recommend selecting an anode material with a high polarity (53). Table 2.1 displays the results of the most extensively researched anode materials. It was found that BDD anodes were the best electrodes. If the raw wastewater has a low chloride concentration, adding a significant amount of salt is necessary in order to enhance the effectiveness of the process (20). In contrast to metal catalytic mediators, for instance, Ag^{+2}, CO^{+3}, and Fe^{+3}, the presence of metal ions could lead to the production of an effluent that is more hazardous than the original effluent. Thus, a separation stage is necessary to recover the metallic species when using this method (54).

Table 2.1 Potential of oxygen Evolution of Different Anodes,V versus NHE.

Anode	Potential (V)	Conditions (mol/L H_2SO_4)
Pt	1.3	0.5
IrO_2	1.6	0.5
Graphite	1.7	0.5
PbO_2	1.9	1.0
SnO_2	1.9	0.5
TiO_2	2.2	1.0
Si-BDD	2.3	0.5
Ti-BDD	2.7	0.5

As a result, there has been an increase in interest in graphite, lead oxide, platinum, iridium oxide, manganese oxide, and titanium dioxide as anode materials. Some of these materials are costly and harmful to the environment, while others degrade to form a polymer coating on the surface of the anode. This is the biggest drawback of these materials.

2.2.2 Cathode reduction

Cathodic oxidation is classified as an indirect oxidation process. Indirect electrolysis is a method employed for the removal of organic contaminants, where chemical agents like hydrogen peroxide are generated. Based on equations 2.11 and 2.12 (41), oxygen can be reduced via the two electrons at the cathode surface in an acidic and alkaline medium, respectively, which can result in the generation of significant quantities of hydrogen peroxide.

$$O_2(g) + 2H^+ + 2e^- \rightarrow H_2O_2 \qquad 2.11$$

$$O_2(g) + H_2O + 2e^- \rightarrow HO_2^- + OH^- \qquad 2.12$$

Hydrogen peroxide is considered one of the largest and most adaptable chemical oxidizing agents for a wide variety of applications, such as bleaching paper, textiles, and wood. It is also used as an oxidizing agent in medical and industrial settings and to clean up wastewater. The reaction doesn't leave behind any harmful chemicals like chlorine-based bleaches, which is good for the environment. Reduction with oxygen produces a large amount of hydrogen peroxide gas. The electrochemical method might be a good alternative to the usual ways of making H_2O_2 (42).

Improving the interactions between the cathode, oxygen, and water is necessary to enhance the performance of H_2O_2 electro-generation. Many researchers have implemented various carbon-porous cathode materials to function as gas diffusion electrodes (GDEs). There were also gauzes, active carbon felt, carbon-nanotube-based PTFE with technical carbon combinations, and reticulated vitreous carbon (RVC). Martínez-Huitle et al., 2015 showed that preferred electrodes might consist of three dimensions and possess a substantial specific surface area (41).

Willyam et al., 2014 discovered that carbon is frequently employed as the cathode material to generate H_2O_2 because it is non-toxic, stable, has a high overpotential for producing H_2, is conductive, porous, chemically resistant, cheap, and doesn't break down H_2O_2 very quickly (55). Lie Zhou et al., 2014 GDEs reported that carbon materials are popular cathodes due to their efficient 2-electron oxygen gas reduction and significant in-situ hydrogen peroxide generation. GDEs, with their porous and hydrophobic features, allow for unlimited oxygen delivery to the electrode/electrolyte contact, making them a unique electrode for increasing H_2O_2 generation (56). Luo et al., 2015 revealed that a GDE's porous shape allows for unlimited gas and chemical flow to the electrode/electrolyte interface, overcoming mass transfer restrictions in the process (57). Hamdan et al., 2022 made a C-PTFE gas-diffusion cathode to increase hydrogen peroxide on-site generation in alkaline solutions (58). In cases where Fe^{+3} salts are added to effluent, an electro-Fenton reaction takes place, as stated in Eq 2.13.

$$Fe^{2+} + H_2O_2 \rightarrow Fe^{3+} + OH^{\bullet} + OH^{-} \qquad 2.13$$

Willyam et al., 2014 investigate the electro-Fenton process with Fe^{2+} and a modified gas diffusion electrode (MGDE) to clean up wastewater from food and drink processing and manufacturing facilities. The inclusion of Fe ions considerably enhanced the process's efficiency. After 90 minutes of electrolysis, a dosage of 0.15 mM Fe^{2+} resulted in the highest decolorization (79.3%) and mineralization (67.3%). The electro-Fenton process with Fe^{2+} and an MGDE is a promising method for degradation in an aqueous medium (55). However, Huanqi et al., 2020 showed the precipitation of Fe^{+3} during electro-Fenton oxidation remains a concern, leading to iron loss. Chain Fenton reactions can produce Fe^{3+} hydration, which can precipitate ferric oxyhydroxide species in oxygen-saturated solutions at high concentrations of iron (II) (30). Even though using electricity can decrease the quantity of iron sludge, Fenton processes will still produce it in the end (59).

2.3 Factors affecting MO removal

2.3.1 Electrode Materials

EO's percentage of removal and effectiveness rest a lot on the type of material used as the electrode, so picking the right one is very important.

Electrode material selection is crucial for process selectivity and efficiency. The material for the electrode must have these properties, as reported by Jasim et al., 2023 (42) :

- high levels of both physical and chemical stability, as well as resistance to both erosion and corrosion, in addition to the creation of passive layers.
- The material which has a high level of electrical conductivity.
- Selectivity and good catalytic efficiency.
- Excellent durability (i.e., extended service life) and low price.

The development of enhanced electrode materials has made significant progress. Researchers are exploring several new substances for anodes, including polypyrrole (60), granular activated carbon (4), activated carbon fiber (ACF) (59), graphite (61,62), platinized Ti and massive Pt, both pure and doped-PbO_2, and mixed metal oxides (MMO) of Ti, Ru, Ir, Sn, Ta, and Sb (63). Numerous studies have provided evidence supporting the significantly higher efficacy of so-called nonactive anodes such as PbO_2 (64,65) and BDD (66).

Additionally, the production method has an impact on the anode's properties. The factors that significantly influence the performance of the anode are the bonding force, particle dimension, surface shape, and composition ratio (42). As a conclusion, different electrocatalytic materials were used to break down different dyes, such as methyl orange (63,67), reactive Brillint Red X-3B (68,69), C.I. Basic Red 29 (64), acid blue and basic brown (35), reactive black 5 (62), and C.I. Acid Orange 7 (4).

2.3.2 Value of pH

The pH value of the solution is a critical operational parameter in EO processes due to the fact that the efficiency of pollutant removal is typically greatest at the optimal pH level, while it decreases as the pH falls below or rises. A literature review reveals varying conclusions regarding the impact of pH on AO and AO-H_2O_2 processes. It should be noted that the utilization of pH values exceeding 2.5 results in significant precipitation of $Fe(OH)_3$ due to the continuous

production of OH^- at the cathode. As a consequence, the system experiences a decline in performance (70).

Ghenymy et al., 2014 found that a number of studies have suggested that mineralization rate independence exists in the pH range of 2.0 to 6.0 (65). However, Segura et al., 2015 found that the process responded more effectively at pH 3.0 than at higher pH levels (71). In contrast, Hamza et al., 2009 reported a significantly quicker rate of mineralization at a pH value of 7.4 in comparison to 3.0 (72). An identical viewpoint by Mittal et al., 2007 discovered that adsorption decreases with rising pH. The neutralization of the negative charge at the adsorbents' surfaces may account for the increased dye adsorption at low pH (73). Qicheng et al., 2018 suggested that an acidic solution with a lower pH was more effective for AO7 dye removal (74). Jianmeng and Yijing., 2015 found that the highest rates of chloramphenicol elimination were reported at a pH of 3, a Figure that was 20.85% more than those obtained at a pH of 11(75).

2.4 Electrochemical flow cells

Various flow systems have been studied for electrochemical flow investigations on dyestuff treatment. The widely utilized approach to degrading organic contaminants via in situ H_2O_2 electrosynthesis is the Electro Fenton (EF) process, which is widely recognized. Xu et al., 2014 showed that they made a graphene-doped gas diffusion cathode (GE/graphite-PTFE GDE) by mixing PTFE and graphite powder. They examined the electrode's function for H_2O_2 electro-generation. The GDE increased the amount of H_2O_2 three times more than the raw graphite-PTFE GDE. After 3 hours at pH 3.0 and 0.75 mmol/L Fe^{+2}, the electro-Fenton method got rid of 33.3% of the Brilliant Blue (KN-R). For their project, they used graphite, which is an expensive material, to make a prepared cathode electrode. But, I used carbon black because it was cheaper than graphite (76).

Banuelos et al., 2014 revealed the utilization of an oxygen diffusion with an activated carbon (AC)-packed cathode for the generation of H_2O_2. The paper found that when eliminating methyl orange (MO) from wastewater at a dosage of 97 mg/L, the generation of hydrogen peroxide (H_2O_2) was 10 times higher than the production of dissolved oxygen (O_2). Used a cylinder-shaped cell with granular activated carbon (GAC) set up as an air diffusion electrode for the

electrochemical tests. The experiments yielded a significant reduction of TOC by 90% and a complete elimination of color within 240 minutes. However, there is a significant disparity in the duration of electrolysis required for the degradation of MO between the referenced work and my own study (77).

Han Yu et al., 2015 reported that both the original TSSA investigation and the TSSA-ADC investigation were conducted in a rectangular plexiglass reactor. Researchers studied the electrochemical degradation of methyl orange (MO) dye in an aqueous solution in both systems. Ti/SnO_2-Sb was used as an anode, while TSSA-air diffusion was used as a cathode. Every experiment was performed utilizing 800 mL of electrolyte at a 15 mL/min discharge rate. The TSSA-ADC system achieved 95% decolorization in 2.5 hours by applying a constant current of 0.5 mA/Cm^2, while the TSSA system almost completely removed MO after 4 hours of operation (78). In my research, I reached the same removal percentage after one hour.

Roth and Gendel., 2015 demonstrated that a tubular electrochemical reactor can eliminate Acid Red 14 from wastewater using cyclic adsorption-electro-Fenton. The MWCNT microtube is an air diffusion cathode and an extremely porous adsorber. The electro-Fenton method degrades pollutants. Full regeneration of adsorption capacity, removal of color, and 50% and 70% clearance rates are achieved. However, this method is appropriate for removing low-polluted water (79).

Thiam et al., 2015 indicated that they used an electrolytic system to remove the color water solutions that contained the food azo dye Allura Red AC and turn them into mineralization. The cylindrical glass, opened at atmospheric pressure, received a double jacket to regulate the temperature to 25 degrees Celsius. The system was constructed up of a 3 cm^2 carbon-PTFE air-diffusion electrode and a 3 cm^2 Pt sheet or 3 cm^2 BDD thin-film electrode for the anode. The experimental outcomes demonstrated that the PEF-BDD was the most effective EAOP in terms of total mineralization and decolorization. At 33.3–150 mA/cm^2, a 96–98% TOC reduction was achieved with 115–460 mg/L of dye (80). This method of treatment utilized chemicals like Na_2SO_4, $LiClO_4$, $NaNO_3$, or

NaCl as electrolytes. Maybe these chemicals led to the formation of sulfate-iron and recalcitrant chloro-derivatives. While I only used KOH.

In another study, Yangming et al., 2015 showed the optimized degradation conditions for brilliant red X-3B in water utilizing a trickle bed reactor (TBR) involving carbon black-PTFE-coated graphite chips to generate hydrogen peroxide. The H_2O_2 concentration was 5.01 mmol/L, the production rate was 134 μmol/(h.cm^2), and the current efficiency was 63.7%. They successfully removed the brilliant red X-3B from water after 1 hour of electrolysis under specific conditions: an initial pH of 3, a cell voltage of 4.5 V, and air and electrolyte flows of 0.1 m^3/hr and 15 mL/min, respectively. They demonstrated that the TBR could efficiently handle low-concentration wastewater or integrate with other treatment units (81). This reactor is not appropriate for high wastewater concentrations.

Labiadh et al., 2016 indicated that their research examined the electrocatalytic characteristics of $TiRuSnO_2$, PbO_2, and BDD anodes for the combustion of methyl orange (MO), an azo dye. The results showed that hydroxyl radicals completely oxidized MO and that high flow rates facilitated elimination. At a starting concentration of 100 mg/L, both BDD and PbO_2 anodes showed almost complete MO degradation after 150 minutes. However, BDD removed more COD than PbO_2, with 96% and 79% minerals, respectively (82).

Liang et al., 2016 conducted that a gas-diffusion electrode (GDE) fabricated using a rolling process and loaded with small amounts of the transition metals (Cu, Ce, Mn, Fe, and Co) was employed as the cathode in a hybrid like electro-Fenton system for the decomposition of methyl orange (MO). The Gas Diffusion Electrode (GDE) worked well and lasted a long time when it came to making hydrogen peroxide (H_2O_2). The Cobalt/GDE showed the most activity at a concentration of 0.7% weight percent and stayed stable at a pH level of 3 (83).

Yang et al., 2016 ICBR and SEBR polymethyl methacrylate reactors with varied operating sizes for the tests. The ICBR used iron shavings as its cathode, soaking them in 5% w/w H_2SO_4 for 20 minutes before rinsing them with deionized water to pH 7. Having regulated electrode distances at 10 mm, the ICBR utilised three rods of graphite and one rod of iron as anode electrodes. The ideal air flow rate under the cathode was 0.1 m^3/min, which led to 95% MO

decoloration efficacy and 0.51 mmol/L H_2O_2. SEBR anodes and cathodes were graphite plates with a 0.75 L working capacity. To provide continuous air under the cathode to evaluate ICBR with SEBR. The researchers changed pH, $FeSO_4$, and Na_2SO_4 to increase the production of hydroxyl radicals. In conclusion, they suggested that utilising the ICBR as a replacement for SEBR can reduce electrical energy usage in the treatment of MO by 85.2%. However, the difference between our work and that of Yang et al. is that we applied a 1 volt power supply instead of a 5 volt one (84).

Li et al., 2017 demonstrated that in their research, they made pure N mono-N/P dual-doped ACF from cotton stalks. They used this as the electrode in the EF process to degrade methylene blue (MB). It was shown in the experiments that the original ACF and the N/p dual-doped ACF both made H_2O_2 at rates of 0.41 mg/(cm^2.h) and 0.25 mg/(cm^2.h). This meant that the N/P dual-doped ACF was 24.1% more effective at removing MB than the original ACF. Based on this, we can say that higher H_2O_2 generation ultimately influences the way EF works (85). Since I just utilized 1 volt instead of his 15 volts, my work is more cost-effective.

Dr. Krishna et al., 2017 showed the elimination of color from synthetic and textile wastewater. They used Fenton oxidation to produce hydrogen peroxide (H_2O_2) by utilizing ferrous ions. Overall, the reported findings indicate that the synthetic wastewater demonstrated a color removal effectiveness of approximately 90.47%, whereas the textile wastewater showed a color removal efficiency of around 72.72%. Therefore, it is possible to infer that the elimination of color from synthetic and textile effluents mostly relies on the dissolution of iron molecules in the Fenton process (86).

Jin et al., 2018 found that using reed straw activated carbon (RSAC) as the cathode resulted in a 93.06% destruction rate of organic pollutants after 120 minutes. The outcomes indicate that the RSAC has a high specific surface area and electrocatalytic activity. The experiment employed electrochemical techniques within a monolithic cell. For effluent treatment, the cell used a locally produced RSAC material as the cathode and a Ti/IrO_2/RuO_2 mesh as the anode. The treatment process involved the use of a 0.1M sodium sulfate solution.

However, the presence of these compounds, namely Na_2SO_4, leads to sludge formation, necessitating frequent maintenance (87).

Márquez et al., 2020 showed that the EF processing of MO streams in a flow plant was more successful than AO treatment due to the increased generation of $OH^{\bullet}$. Under the best circumstances, the PEF system accomplished complete color removal and 94% TOC abatement by continuously regenerating a Fe^{2+} catalyst. The oxidation power of the PEF system with a 3D-like GDE is adequate for treating azo dyes in water. However this process needs to be acidic and controlled because it was carried out at 3 pH. In my study, the reaction occurred in an alkaline solution without the need for other chemicals (88).

Henrique et al. 2020 revealed how well an EF system with a modified gas diffusion electrode could turn wastewater from textiles into hydrogen peroxide (H_2O_2). Graphene oxide (rGO), which supports magnetic nanoparticles, was employed as a highly efficient, heterogeneous Fenton-like catalyst to accelerate the process. The anode employed was made of stainless steel, while the cathode utilized a gas diffusion electrode (GDE) with an overall surface area of 18.84 cm^2 (89).

Elbatea et al., 2021 conducted the electro-Fenton technique in a batch reactor using a cylindrical plexiglass column of 24 cm in height and 9.4 cm in width. To ensure a consistent and even flow of oxygen from a cylinder, the base of the reactor connected to a sintered glass component. The cathode chamber consisted of a permeable stainless steel basket with a diameter of 9.3 cm. Several graphite layers made up the cathode chamber. Every layer is comprised of 69 tiny graphite cylinders. The sacrificial anode is comprised of five horizontally aligned low-carbon steel screens, with each screen having a diameter of 9.3 cm. The electrical circuit comprised a direct-current power supply and a voltage regulator. To completely get rid of Reactive Red 195 from a solution that has 50 ppm of dye in it at the start, the best conditions are 2 mA/cm^2 of current density, 0.012 cm/s of O_2 gas velocity, and 60 minutes of residence time (90). The general perspective for the removal of various types of dyes was clearly and comprehensively shared in Table 2.2.

Table 2.2 General perspective for removal of dyes using electrochemical oxidation.

Pollutant	Wastewater characteristics	Process	Operational parameters (Maximal Removal decay)	Ref
Reactive Red 195	(100-400) mg/ L Na_2SO_4:0.1 M	EO	Anode:Ti/SnO_2–Sb/PbO_2 Cathode:4-chloro-3-methyl phenol (CMP) E: (5- 40) Ma/ cm^2 pH: 2.0, 5.6, 15 , T: Amb TOC (80% - 53%)	(93)
Acid Orange 7	(7.0- 14) g/ (1.4-18) L Na_2SO_4 or (6.1-12)g/ $NaClO_4$ L or 2.9 g / NaCl L	EF	Anode: Pt (1 cm^2) Cathode: Graphite felt (3.8-7.6 cm^2) E: (0.5-1.0) V T: Amb , pH: 3.0 (75%)	(92)
Basic Blue 3	0.2 mM BB3 0.1 M $NaNO_3$	EF EC	cathode: Carbon sponge and carbon felt E:(30-200) mA T:25°C , pH:3.0 O_2 flow rate: 100 ml/min TOC(91.6% , 50.8%)	(59)
Orange II	50 mg /L in 7.0 g Na_2SO_4 /L	AO-H_2O_2 EF PEF-UVA	Anode: Graphite cloth (200 cm^2) Cathode: Graphite cloth (164 cm^2) jcat: E : 300 mA /cm^2 ,Q: 0.1 L/ min ,T: Amb. pH: 3.0 (80% – PEF-UVA)	(40)
Methyl orange	20 mg/L 31 g /L NaCl	EO	Anode:Ti/SnO_2-Sb Cathode: TSSA-ADC E : (0.5-15) Ma/cm^2, pH:6 T: 25°C (95%) removal ratio	(78)
Methyl orange	30 mg /L . Na_2SO_4: 0.08 mol /L	EO	Anode: Nb/PbO_2 Cathode: graphite E:50 mA/cm^2, pH:6.0, T: 45°C, Color removal (99.6%) and COD (72.6%)	(94)
Methyl orange	50 mg/L Na_2SO_4:0.1 mol/L	EC	Anode:Ti/IrO_2/RuO_2 Cathode: self-made Pd/C E: 39 mA/cm^2 pH:7.0, T: Amb TOC (89.3%)	(91)
Methyl orange	50 mg /dm^3 0.050 or 0.50 mol/ dm^3	AO EC	Anode: Ti/Ir–Pb, Ti/Ir–Sn, Ti/Ru–Pb, Ti/Pt–Pd or Ti/RuO_2 cathode: Ti/RuO_2, Ti or 316 stainless steel T: 25 °C , pH:7.0 Color removal (96%,84%,81%)	(63)

Zhili sun et al. 2022 conducted a comparative analysis of perforated 3DER and 2DER systems for the purpose of eliminating methyl orange. The reactor was made using a 2 cm-diameter graphite rod as the anode and a stainless-steel mesh (0.4 mm wire diameter, mesh number 12). The area between the cathode and anode is filled. A mixture of granular activated carbon (GAC) and quartz sand (volume ratio 4:1) as the third electrode is the only difference between them. They found the methyl orange removal was 79.5% with a voltage applied of 1.0 V, a distance between electrodes of 2 cm, and an initial MO concentration of 60 mg/dm^3. This is greater than the 58.8% achieved in the 2DER, meaning that the reduction of MO by the 3DER is 20.7% greater than that of the 2DER (2). In contrast, I achieved that percentage removal at 100 ppm.

There are some big problems with the electro-Fenton method, like the fact that it needs to be used in low pH conditions and that dissolved iron has to be separated before it can be treated and removed. Additionally, the complex design of the GDEs is another difficulty for contemporary electro-Fenton devices. Typically, planar GDEs are made up of an extremely organized catalyst layer and an open porosity gas diffusion layer (79). In order to surmount these constraints and circumvent complications associated with both GDE and TBR, a gas diffusion electrode was implemented within a TBER reactor to generate enhanced hydrogen peroxide and obtain an adequate concentration of H_2O_2 for the purpose of on-site oxidation of organic pollutants.

3. HYPOTHESES, MOTIVATIONS, AND OBJECTIVES

In this thesis study, the following hypotheses (H) were determined as the driving forces that made the research need to be investigated and put forward.

H1) In the present study, the increasing voltage was expected to lead to a significant increase in MO removal.

H2) In the current study, an increase in reaction temperature may lead to an increase in MO removal.

H3) Among similar AOPs, TBER including of C-PTFE gas diffusion electrode may contribute to the descending activation energy and this may be result in an increase in MO removal in the study.

H4) Considering the outcomes of the related literature and the results of the primary runs of the present study, it can be highly considered to observe that a reasonable decrease in MO removal may occur under O_2-absent conditions.

To test and validate the hypotheses given above, the following motivations (M) were determined as the ways to test whether the proposed hypotheses were significant or not.

M1) To test H1, utilization of a UV-based spectrophotometric method was determined as a reasonable way to investigate the change in removal of MO.

M2) To investigate H2, experiments at various temperatures were planned to be set. Depending on the MO removal, H2 may be tested by calculating the kinetic parameters.

M3) To check out H3, the activation energy of C-PTFE gas diffusion electrode-included TBER process may be calculated and compared with the results of related literature concurrently.

M4) To justify H4, the experiments under the conditions of absence and presence of O_2 may be performed and compared with each other.

Considering the whole hypotheses and motivations of the present study, the objectives (O) to be criticized can be listed as follows:

O1) Design of a novel reactor including a specific catalyst in gas diffusion electrode to fill the gap in related literature in terms of oxidation-based degradation.

O2) Utilization CB-PTFE as a catalyst located onto stainless steel meshes for generation of further H_2O_2 demanding no other chemicals.

O3) Investigation of the effects of the explanatory variables of temperature (T, °C), voltage (V, volt), initial MO concentration (IMOC, ppm), electrolyte concentration (EC, M), and flow rates of electrolyte (FRE, mL/min) and oxygen (FRO L/min)

O4) For maximization of MO removal, determination of optimized conditions and validation of these optimized conditions.

O5) Determination of the kinetic parameters to demonstrate the way how MO degrades depending on the temperature change.

4. MATERIALS AND METHODS

The electrochemical degradation behaviours of the model azo-dye (methyl orange) on carbon electrode for gas diffusion by trickle bed electrochemical reactor (TBER). And prepared the carbon black (CB)/(PTFE) catalyst bed and examined methods.

4.1 Materials and Chemicals

4.1.1 Chemicals

Methyl orange (MO) dye and potassium hydroxide (KOH: purity 85%) were purchased from Alpha Chemicals India, SDFCL s d fine Chem Limited, Chennai- India respectively. The chemical structure of MO is shown in the Table below. All solutions were prepared with deionized water.

Table 4.1 Properties of methyl orange (95).

Properties	Value
Molecular formula	$C_{14}H_{14}N_3NaO_3S$
IUPAC name	Sodium 4-[(4-dimethylamino) phenyldiazenyl] Benzenesulfonate
Chemical/Dye class	Azo type/Anionic dye
Absorption band	485 nm
Molar mass	327.33 g/mol
Melting point	> 300 °C
Density	1.757 g/cm^3
Solubility	Slightly soluble in water
Physical form	Orange-yellow powder

4.1.2 Analysis apparatus

The concentration of methyl orange is analyzed using a UV-Vis spectrophotometer with double beam technology (UV-1800, Shimadzu/Japan) from Tikrit University's College of Engineering. Using to evaluate the methyl orange content in liquid samples.

4.1.3 Methodology and Analysis

The absorbance (A) decline of treatment MO dye solutions was evaluated by analyzing spectra obtained at various time periods at 465 nm with a UV-1800 double beam spectrophotometer (Shimadzu, Japan). The following formula was used to determine the percentage of organic pollutant removal or removal efficiency (%):

$$Re\% = \frac{A_0 - A_t}{A_0} \times 100 \qquad 4.1$$

A_0 and A_t indicate the absorption values of MO at the start time and time t, respectively, at a wavelength of 465 nm (63). To evaluate the removal of MO, we used a standard absorbance against time.

4.1.4 Catalyst

Carbon black and Polytetrafluoroethylene (PTFE) at a ratio of 2:1 were used to create the catalyst bed. The physical properties of powder form of carbon black (Vulcan XC-72) and (PTFE) were illustrated in Table 4.2 and Table 4.3, respectively.

Table 4.2 Physical properties of CB.

Physical properties	Value
Bulk density (kg/m^3)	96
Particle size (nm)	50
Surface area (m^2/g)	250

Table 4.3 Physical properties of polytetrafluoroethylene.

Molecular formula	$(CF_2CF_2)_n$
Dispersed in water	60 wt%
The density of dispersed (kg/m^3)	1510
Particle size (μm)	0.2
pH	9.5-11

4.2 Catalyst bed

The catalyst bed was made using two main materials (CB-PTFE) first time by Abdulla (2017) (96). Figure 4.1 illustrates the catalyst block after the fabrication.

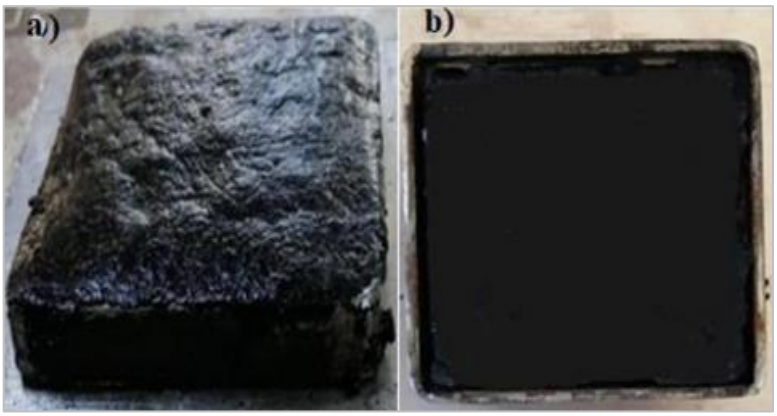

Figure 4.1 CB-PTFE catalyst blocks (a) before calcination, and (b) after calcination.

4.3 Experimental Setup

The TBER developed was used to degrade methyl orange in situ with hydrogen peroxide. Figure (4.2) shows the wastewater treatment process equipment, and Figure (4.3). illustrate the flow diagram process.

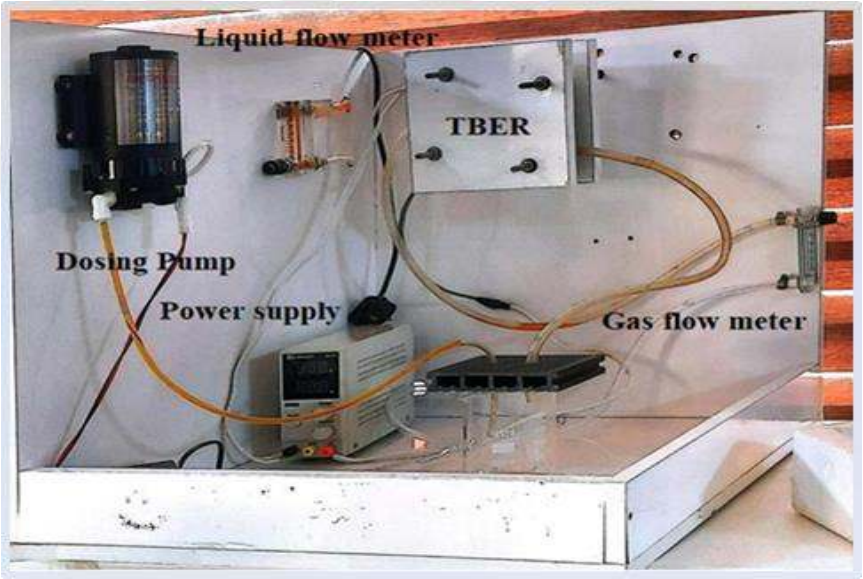

Figure 4.2 Experimental setup.

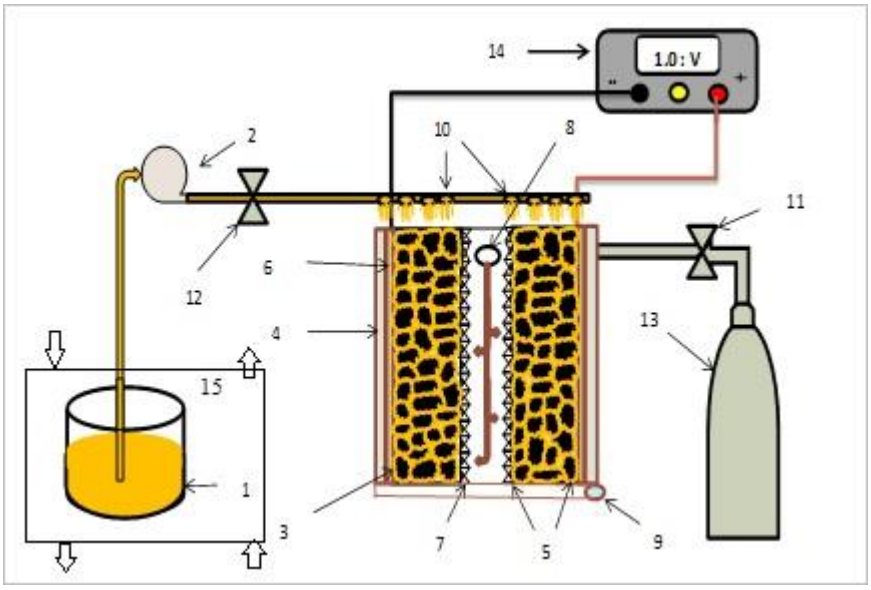

Figure 4.3 Schematic flow diagram of experimental of the processes:1- Synthetic wastewater (MO), 2- Dosage Pump, 3- CB-PTFE, 4- Anode electrode, 5- Cathode electrode, 6- Membarance, 7- Mish, 8- Inlet for oxygen, 9- The Outlet, 10- Wastewater and electrolyte inlet, 11- Oxygen flow meter, 12- effluent flow meter, 13- Oxygen source, 14- power source, 15- water coolant cycle.

4.3.1 Trickle Bed Electrochemical Reactor (TBER)

The device below is composed of a TBER that is coupled with a gas diffusion electrode. The pieces of the TBER reactor before implementation are illustrated in Figure 4.4. The majority of these elements were locally designed.

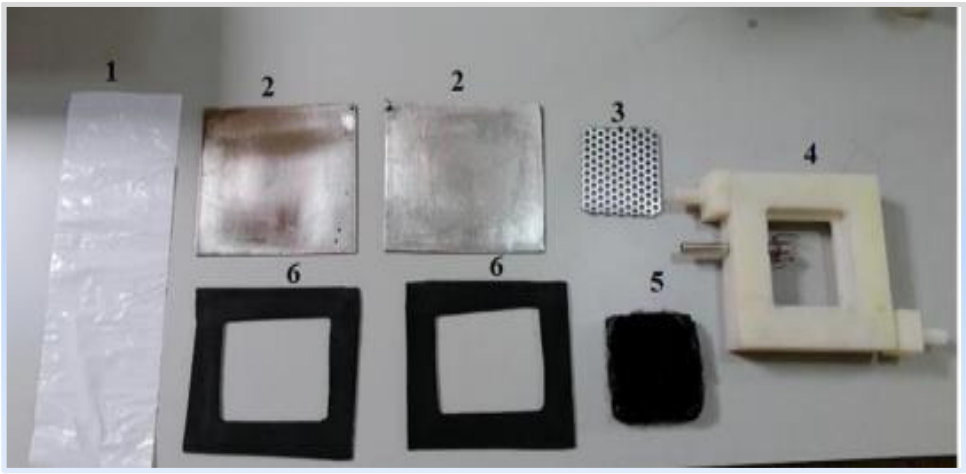

Figure 4.4 The TBER parts: 1- Celgard membrane, 2- Stainless steel plates, 3- Stainless steel meshes, 4- Cathode frame, 5- C-PTFE block, and 6- Rubber rings.

The trikle bed electrochemical reactor was comprised of six parts, as illustrated in Figure 4.4. A cathode frame was made from a solid structure with two inlets with dimensions of (120×110×40) mm (width, height, and

depth), a C-PTFE block was placed as a cathode, the anode electrode consisted of two pieces of stainless steel plates with 70 mm × 60 mm (width and height) were placed on both sides of the reactor. Furthermore, in order to prevent a short circuit from occurring, a Celigard membrane was positioned between the cathodes and the anodes on each side. The TRBE is constructed by arranging all of these components and then tying them into two separate plastic pieces. The Celgard membrane is microporous and has a highly efficient membrane. Advantages of the coating include heat resistance, adhesion, and surfactant. It can be utilized in many applications, such as electric drives, energy storage, and specialty batteries.

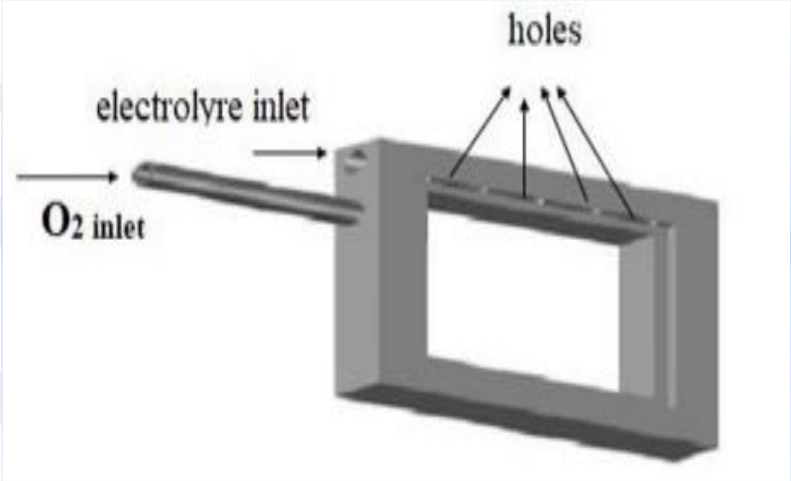

Figure 4.5 Oxygen inlet and KOH inlet in cathode frame schematic diagram.

The cathode has a solid structure, as shown in Figure 4.5. The liquid containing methyl orange with the electrolyte (KOH) flows to the cathode framework from the top and is split into two rows, each row contain four holes on its side, for the suitable liquid distribution in both ways over the catalyst layer, at the same time, the oxygen gas is fed to the cathode framework reactor to the chamber located between the two stainless steel grids to spread directly in the channels of the CB-PTFR catalyst layer to obtain super gas diffusion, one exit for discharge all material reactant or product from the bottom of the cathode framework. This design was developed to get around the oxygen solubility issues in electrolyte solutions that plague conventional electrodes (58), allowing for a greater amount of oxygen to diffuse through the bed, resulting in increased H_2O_2 synthesis, which in turn leads to increased oxidation of methyl orange, allowing for its simple removal. The whole piece is safely

enclosed between two plastic pieces measuring 170 mm× 170 mm (width, height). Figure 4.6 depicts a schematic configuration of TBER pieces.

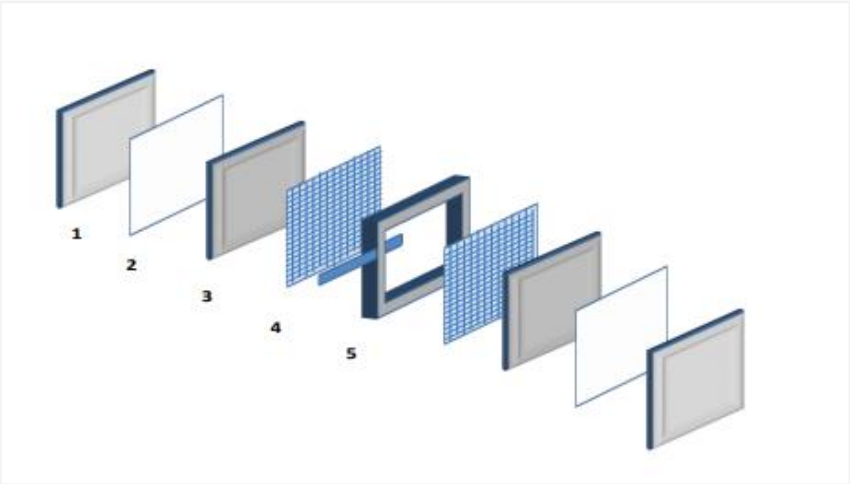

Figure 4.6 TBER parts are represented in a diagram: 1. The cell structure, 2. Celgard layer, 3. The C-PTFE block, 4. The stainless steel mesh, and 5. The cathode framework.

4.3.2 Methyl orange oxidation mechanism

At the beginning, the appropriate concentrations of electrolytes (KOH) and methyl orange (MO) were combined in the beaker (500 ml), and the ambient temperature of the TBER reaction was regulated through water exposure. A liquid flow meter was utilized to control the flow, and a dosing pump was used to release the waste. The compressed gas cylinders provided the O_2, and the gas flow meter managed the oxygen flow. The top of the TBER was used to supply MO and KOH, while the side was used to supply O_2. The reactor was activated to generate hydrogen peroxide at the necessary voltages. The procedure for the creation of hydrogen peroxide and MO oxidation in TBER is illustrated in Figure 4.7, which shows the electrochemical formation technique.

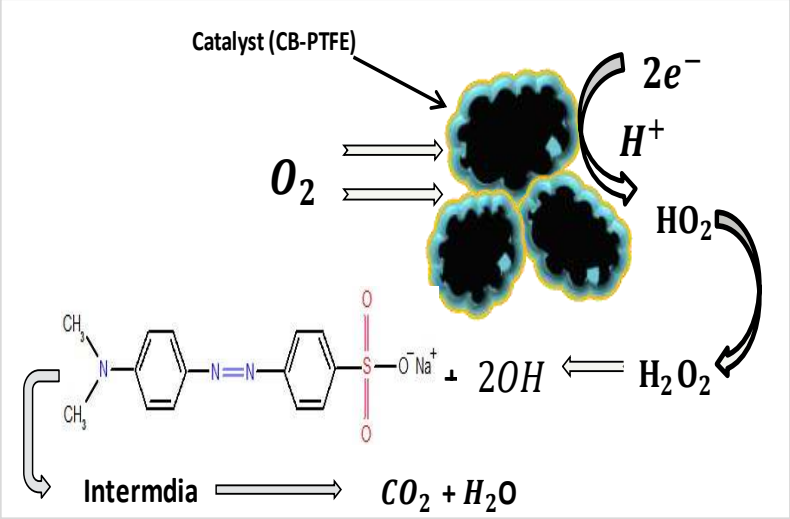

Figure 4.7 Diagram showing the electro-generation of hydrogen peroxide and MO dye elimination on the C-PTFE.

.

4.4 Levels of the operating parameters

All the levels of operating parameters of initial dye concentration, voltage, KOH concentration, oxygen flow rate, KOH flow rate, and temperature were investigated in the present study (Table 4.4).

Table 4.4. Levels of operating parameters.

Operating parameters	Symbols	Unit	Levels
Initial dye concentration	IDC	ppm	20, 40, 60, 80, 100
KOH concentration	KOHC	mg/L	0.2, 0.4, 0.6, 0.8, 1.0
KOH flow rate	KOHF	mL/min	50, 100, 150, 200 ,250
O_2 flow rate	FR	mL/min	3, 5, 7, 9, 11
Voltage	V	V	0.5, 1, 2, 3, 4, 5
Temperature	T	^oC	5, 10, 20, 30

4.5 Execution of the experiments

4.5.1 Calbriation curve

Two calibration curves were constructed at 465 nm, each one with 5 concentration levels ranging from 2 to 10 ppm and 20 to 100 ppm, to determine the amount of methyl orange removal in the experiments. The analytical parameters of working calibration curves are shown in Appendixes.

4.5.2 Experimental steps

Before beginning, turn on the pump for about 10 minutes at the highest flow rate to examine it for any potential leaks. In the second step, TBER was washed with ethanol to dissolve any residue after the experiment was complete. Upon completion of each experiment, the TBER is cleaned several times with deionized water to prepare it for the next experiment. Then, the water and pure gas flow meter feeds were controlled to get the appropriate flow rate of liquid and oxygen. Additionally, ensure that the reactor is connected to the power source properly. The electrolyte is added to the wastewater, which contains methyl orange, to get it ready for the experiment.

The steps of the experimental procedure consist of :

1- Using a magnetic stirrer at 100 rpm for 10 minutes, 4.48 g of potassium hydroxide (KOH) containing the methyl orange solution stock in deionized water was dissolved in 400 ml to prepare for the experiment.

2- MO waste is fed to the TBER by a dosing pump and controlled to the flow rate (waste and electrolyte) by a liquid flow meter.

3- A gas flow meter was used to regulate the amount of oxygen pumped into the reactor.

4- The power source controls the voltage and conducts directly it to the reactor. It plays an essential role in the oxidation of MO by combining with oxygen to make H_2O_2.

5- The processes were working in continuous mode. All operating variables are controlled by their own keys.

6- After every ten minutes, an experimental sample of wastewater was drawn and examined with UV-VIS spectrophotometry.

4.6 Kinetic and thermodynamic studies

In the current work, a kinetic component was finished to concentrate on the methyl orange oxidation mechanism. The experimental runs for the kinetic study were performed under various temperatures of 5, 10, 20, and 30°C, voltages of 1V, KOH concentration and flow rate are 0.2 M and 200 ml/min, respectively; oxygen flow rate is 7 L/min; and MO concentration is 100 ppm. As clearly shared

in Table 4.5, electrochemically produced radicals on the surface of the double-layer cathode speed up MO oxidation and degradation.

To define the binary interaction between reaction rate constant and activation energy, Arrhenius equation was used as follows:

$$K = A\, e^{-\frac{Ea}{RT}} \qquad 4.2$$

Table 4.5 The experimental runs of the kinetic study.

Run	T (°C)	RT (min)	Run	T (°C)	RT (min)
1	5	10	13	20	10
2	5	20	14	20	20
3	5	30	15	20	30
4	5	40	16	20	40
5	5	50	17	20	50
6	5	60	18	20	60
7	10	10	19	30	10
8	10	20	20	30	20
9	10	30	21	30	30
10	10	40	22	30	40
11	10	50	23	30	50
12	10	60	24	30	60

RT: Reaction time, T: Temperature.

where Ea is the rate of activation energy (J/mol), T is the temperature of the reaction (K), A is the Arrhenius constant, and R is the gas constant (J/mol/K). The process of oxidation can be described as follows:

$$\text{methyl orange} + H_2O_2 \rightarrow \text{products} \qquad 4.3$$

The response rate is expressed by the following formula, assuming a first-order reaction (n = 1), then the Eq will be:

$$-r_{mo} = -\frac{dc_{mo}}{dt} = k\, C_{mo}^{n} \qquad 4.4$$

where r_{mo} corresponds to rate of reaction (mol/L/s), C_{mo} corresponds to initial concentration of MO (mol/L), and the reaction's order is denoted by n, and the rate constant is k, which is 1/min.

The thermodynamic variables are crucial for understanding the impact of temperature on the process of adsorption and determining whether it occurs naturally. The parameters include changes in enthalpy (ΔH°), entropy (ΔS°), and

Gibbs free energy (ΔG°). The following formula can be used to express these thermodynamic parameters:

$$\Delta G^\circ = -RT\ln K_e \qquad 4.5$$

$$\ln K_e = \frac{\Delta S^\circ}{R} - \frac{\Delta H^\circ}{RT} \qquad 4.6$$

5. RESULTS

Utilizing TBER, the ORR in the reactor produced H_2O_2 in situ, while various process variables were in play to assess the elimination of methyl orange from synthetic waste. In this chapter, the effect of various process factors on the oxidation of methyl orange. Moreover, the kinetic parameters are influenced by the operating circumstances.

5.1 The effect of operational variables on methyl orange oxidation.

5.1.1 The influence of the applied cell voltage.

The effects of voltage applied on methyl orange oxidation were investigated. A summary of the experimental data can be found in Appendix 2, Table 8.2.

Using different operating conditions, we looked at how the cell voltage affected the removal of MO dye waste in the TBER. The results, shown in terms of treatment time, are shown in Figures 5.1 and 5.2.

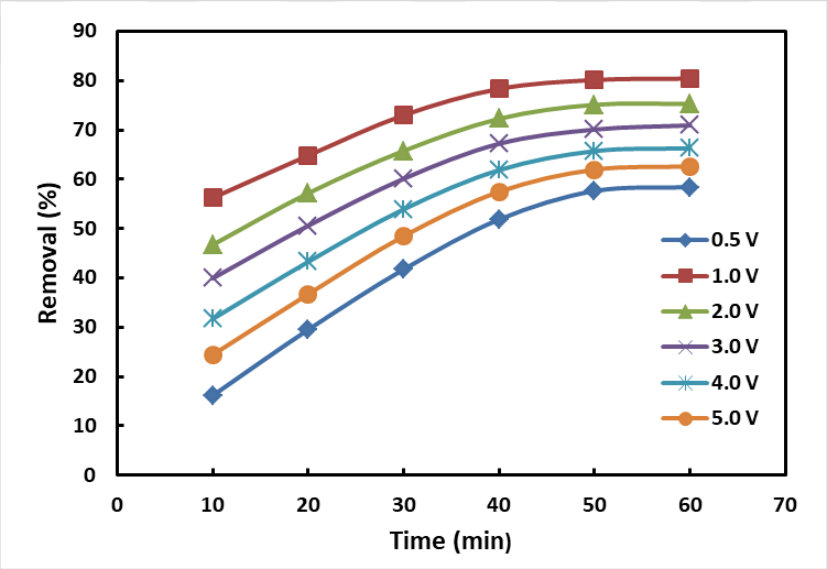

Figure 5.1 Impact of applied cell voltage (0.5, 1, 2, 3, 4, and 5 V) on methyl orange elimination over time at 10 ppm MO, 0.4 M KOH concentration, 3.0 L/min flow rate of O_2, 200 mL/min flow rate of electrolyte, and temperature at 30°C.

The influence of the voltage on the efficacy of MO elimination by using TBER was significant increase to 80.4% from 58.4% has been observed when the voltage was increased to 1.0 V from 0.5 V. Moreover, the results indicate that the

MO elimination efficiency consistently increases in a linear manner until it reaches upto 50 min when it becomes stable. Conversely, a certain decline was noted in MO removal when the voltage rose above 1 V. Applying voltages over 1V clearly led to the form of some specific side reactions and resulted in a vast number of intermediate products than was generally expected (3). As shown in Equation 5.1, using an excessive voltage during electrolysis can cause side reactions, including the creation of H_2O at the cathode.

$$H_2O_2 + 2H^+ + 2e^- \rightarrow 2H_2O \qquad 5.1$$

These secondary reactions may reduce hydroxyl radical formation. Furthermore, it is important to highlight that the effectiveness of removal declines when the voltages are increased from 2V to 5V. This indicates that these increased cell voltages result in the creation of byproducts that have a detrimental effect on the process. Under these circumstances, the production of more kinds of intermediates than anticipated most likely contributes to the decline in efficiency (3,97).

Furthermore, a decline in H_2O_2 formation may explain the drop in MO elimination at cell voltages greater than 1.0 V. The application of a greater voltage to the cell is likely to trigger several additional reactions, for instance, at the anode, H_2O_2 is oxidized to oxygen, which occurs as a result of the creation of $HO_2^{\bullet}$ (98). Concurrently, a two-electron process, or the reduction of peroxide ions on the cathode bed, can quickly convert H_2O_2 into $OH^{\bullet}$ (99). As demonstrated in Eq. (5.2), it is expected to produce of H_2O_2 to undergo a chemical conversion into O_2 both in the medium and at the anode. One of the most important contributors of this part was that the anode would oxidize H_2O_2 to HO_2 (100). by following the ways expressed in Eq. (5.3) and (5.4) (101).

$$H_2O_2 \rightarrow H_2O + \frac{1}{2}\,O_2 \qquad 5.2$$

$$H_2O_2 \rightarrow HO_2^{\cdot} + H^+ + e^- \qquad 5.3$$

$$HO_2^{\cdot} \rightarrow O_2 + H^+ + e^- \qquad 5.4$$

Figure 5.2 illustrates how MO in-situ oxidation occurs under steady operating conditions with a constant response time of 60 minutes. An important

step in this process was applying 1 V, This resulted in the highest production of hydrogen peroxide, which in turn led to the greatest dye removal effectiveness. This could make it easier to get rid of MO because breaking down H_2O_2 could lead to more $OH^{\bullet}$ being made by the electron-transfer reaction shown in Eq. (5.5).

$$H_2O_2 + e \rightarrow OH^- + OH^{\cdot} \qquad 5.5$$

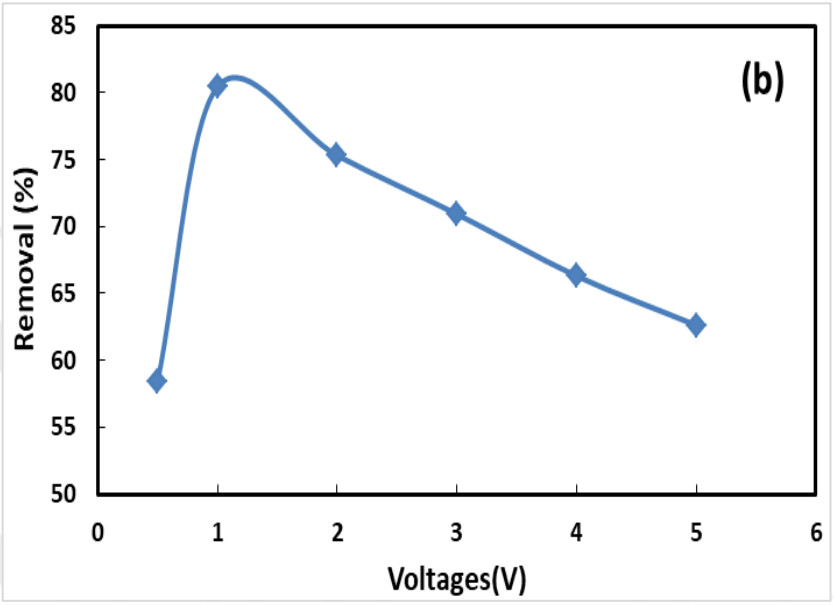

Figure 5.2 The study examines the behavior of the MO elimination at constant operating parameters of 100 ppm MO, 0.4 M electrolyte, 60 min, 3.0 L/min O_2 flow rate, 200 mL/min electrolyte flow rate, and 30°C as a function of the applied cell voltage.

5.1.2 Electrolyte Concentration Effect

TBERs effect on MO in situ oxidation was analyzed through an impact study on electrolyte concentration. The parameters were as follows: 1 V applied voltage, 200 ml/min electrolyte flow rate, 7 L/min oxygen flow rate, and 30 °C reaction temperature. The results were tabulated in Table 8.2 (Appendix 2).

Improving elimination efficiency and up treatment were the main goals of our study, which led us to choose KOH as the supporting electrolyte. This choice was informed by prior research (102). We performed studies demonstrating the oxidation of MO in TBER in the concentration range 0.2-1.0 M under continuous operating conditions.

The impact of the electrolyte concentration on MO elimination efficiency by utilized TBER was clearly decreased to 39.7% from 65.09% when the electrolyte concentration was increased to 1.0 M. Figure 5.3 shows a linear trend for all application cases, with elimination efficiency increased over time during the first 50 min.

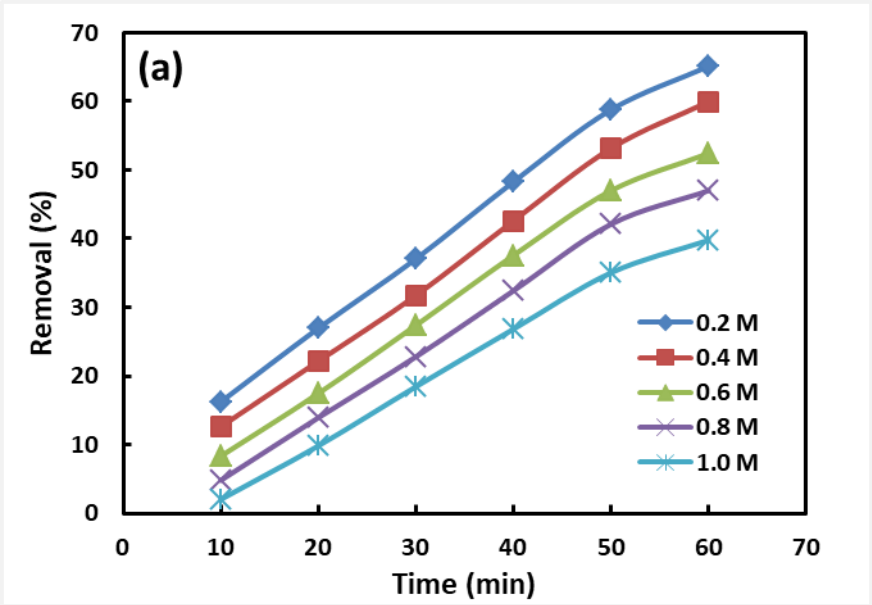

Figure 5.3 The impact of KOH concentration (0.2, 0.4, 0.6, 0.8, and 1)M on MO elimination over time at 1.0 V, 100 ppm MO, 200 mL/min flow rate of electrolyte 7.0 L/min flow rate of oxygen, and 30°C.

Thereafter, removal rates increase slightly, indicating continued elimination activity over time. However, the increase in electrolyte content during MO elimination had the opposite effect. Specifically, The MO elimination efficiency reached its highest point at 0.2 M, achieving 65% at a starting MO concentration of 100 ppm. After that, the effectiveness of MO elimination dropped as the electrolyte concentration rose. The injection of electrolyte into MO wastewater has resulted in an increase in the solution's electrical characteristics and a decrease in cell voltage.(103), thereby increasing mass transfer rates (104). Thereafter, this led to a rise in MO decomposition, as illustrated in Equation (5.6) (91,94,102).

$$C_{14}H_{14}N_3NaO_3S + OH^{\bullet} \rightarrow \text{Intermediates} \rightarrow CO_2 + H_2O \qquad 5.6$$

Pang et al. discovered that, beyond a certain concentration, raising the electrolyte concentration had no noticeable effect on the effectiveness of organic

compound elimination (2,105). It was happening because there were more active notices on the electrode's surface, which inhibited hydroxyl radicals. Based on Equations (5.7) and (5.8) (41). The anode of the electro-generated H_2O_2 could be oxidized to O_2, which would lower the production of radicals like $HO_2^{\bullet}$ and $OH^{\bullet}$ (94). Because of this reduction in radicals, MO elimination decreased.

$$4OH^- \rightarrow 2H_2O + O_2 + 4e^- \qquad 5.7$$

$$2H_2O \rightarrow 4H^+ + O_2 + 4e^- \qquad 5.8$$

The effect of KOH concentration on MO oxidation under constant operation conditions is in Figure 5.4. The results make it abundantly evident that the supportive role of KOH concentration was examined, and that the ideal KOH concentration for attaining it was discovered that 0.2 M had the maximum MO elimination rate.

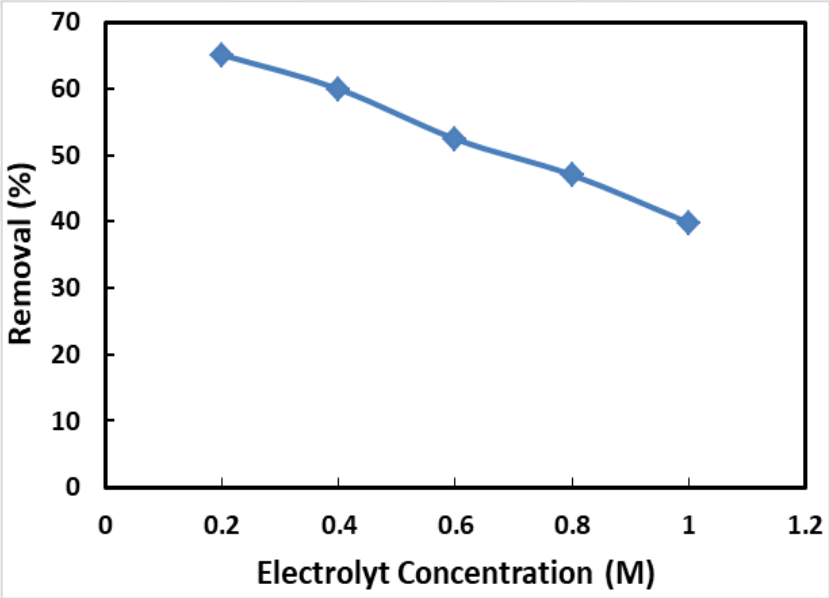

Figure 5.4 Behaviour of MO elimination as a result of KOH concentration under constant operating conditions, specifically at 30°C, 1.0 Volt, 7.0 L/min gas flow rate, 200 mL/min KOH flow rate, and 100 ppm MO for one hour..

5.1.3 Effect of Oxygen Flow Rate

The impact of oxygen flow rate on the removal of methyl orange oxidation in reactor was studied. The flow rates of oxygen tested were 3, 5, 7, 9, and 11 L/min, while the applied voltage was maintained at 1V. The electrolyte concentration was set at 0.2 M, and the electrolyte flow rate was maintained at 200 ml/min. The temperature was kept at 30 ℃ and the amount of methyl orange

was 100 ppm. The experimental data can be found in Table 8.2 (Appendix 2). Previous research has demonstrated that the rate at which oxygen is supplied can have a significant impact on the decomposition of organic contaminants in trickling bed electrochemical processes when peroxide of hydrogen is utilized in situ (42,101). Figures 5.5 and 5.6 demonstrate the impact of the oxygen flow rate supply on MO elimination in the trickle bed electrochemical reactor.

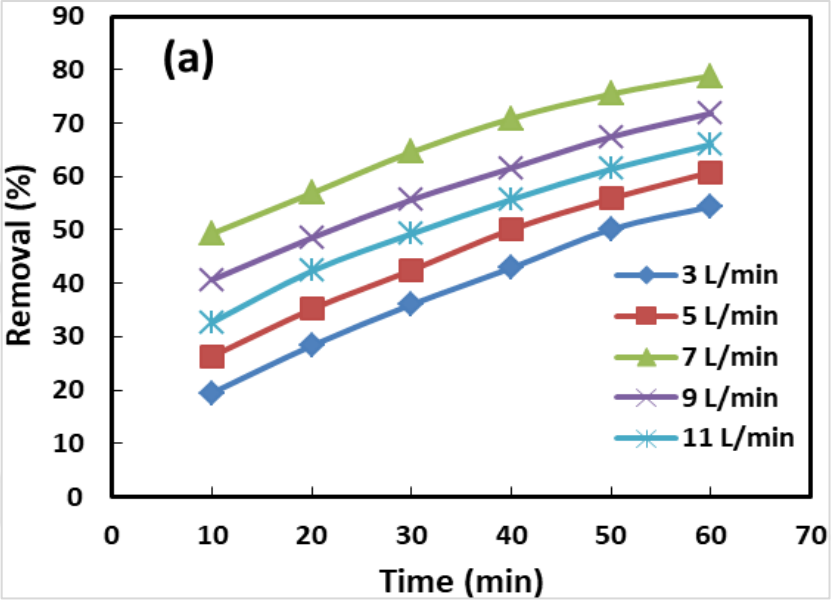

Figure 5.5 The influence of different oxygen flow rates (3, 5, 7, 9, and 11) L/min on MO elimination effectiveness under constant working circumstances of 100 ppm Methyl Orange, 0.2M electrolyte, 60 min, 200 mL/min flow rate of electrolyte (KOH), 1.0 V, and 30°C.

The effect of oxygen flow rate on MO elimination efficiency using TBER was clearly seen to rise from 54.3% to 78.8% when the oxygen flow rate was raised from 3 L/min to 7 L/min. whereas MO elimination efficiency decreased to 66.0% when the oxygen flow rate was raised to 11 L/min. According to the data, the effectiveness of removal rises as the flow rate of O_2 rises, while keeping the operating parameters constant. The maximum elimination efficiency of 78.8% is achieved at 7 L/min flow rate of oxygen. The improvement in the rate of elimination is attributed to the greater formation of H_2O_2 in the presence of additional oxygen, This results in the production of a significant amount of hydroxide radical (58). However, the percentage of MO removal begins to fall if the oxygen flow rate is increased even further than 7 L/min. The reason behind

this is that when the oxygen supply is rosed, it causes a decrease in the liquid level within the reactor. Therefore, both the hold-up and the layer thickness on the bed area get smaller. Higher oxygen transfer at the liquid-solid contact makes it possible for more oxygen to be removed at the cathode, which in turn limits H_2O_2 from forming. In addition, increasing the oxygen flow rates can help to minimize the amount of liquid held up, decrease the wetted bed region, and reduce the active specific surface area. These factors all lead to a decrease in the generation of hydrogen peroxide (101,106), this then reduces the efficacy of MO elimination.

These results highlight the significance of keeping optimal flow rates of pure O_2 in the cathode to guarantee gas-saturated fluids and appropriate hydrogen peroxide electro-formation (107) for high MO elimination.

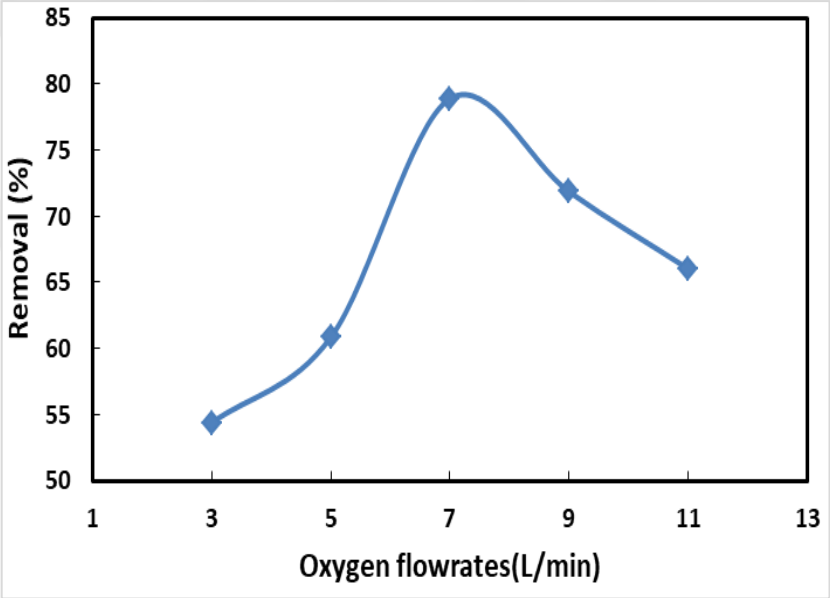

Figure 5.6 MO elimination as a result of oxygen flow rate at 1 volt, methyl orange concentration of 100 ppm, KOH concentration of 0.2 M, and electrolyt flow rate of 200 mL/min; temperature of 30°C.

5.1.4 Influence of the Electrolyte Flow Rate

We investigated the effects of the modified TBER electrolyte KOH dosage on MO oxidation elimination efficiency. We looked at a variety of flow rate, including, 50, 100, 150, 200, and 250 ml/min. A 1 V applied voltage, a 0.2 M electrolyte concentration, a 7 L/min oxygen flow rate, a 100 ppm MO concentration, and a 30°C reaction temperature are the parameters employed in the experiment. The outcomes of the experiment were displayed in Table 8.2,

Appendix 2. Figure 5.7 shows how the electrolyte's flow rate affects the elimination of MO in the reactore.

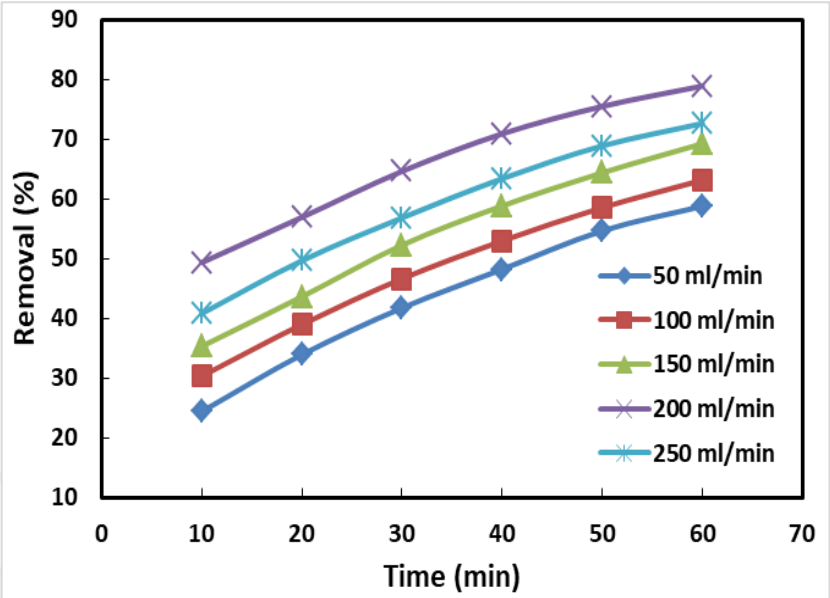

Figure 5.7 The influence of increasing KOH flow rates (50, 100, 150, 200, and 250) mL/min on the effectiveness of MO clearance over time under constant operating circumstances (7.0 L/min oxygen flow rate, 100 ppm MO, 1.0 V, 0.2 M KOH, 60 minutes, and 30°C).

The impact of the electrolyte dosage on MO elimination efficiency by using TBER appeared clearly increased to 78.7% from 58.7% when the rate of electrolyte flow was raised to 200 ml/min from 50 ml/min. The experimental data indicates a positive correlation between the increase in KOH flow rate and the improvement in MO elimination effectiveness. The maximum elimination efficiency of MO is 78.8%, which is attained when the flow rate is set at the ideal value of 200 mL/min. The increased efficiency of eliminating MO at greater rates of flow may be attributed to the link between a raised fluid flow rate and the creation of more H_2O_2. Increased H_2O_2 generation leads to better MO removal. Nevertheless, when the rate of flow exceeds the recommended value, there will be a decrease in the efficiency of elimination at 72.6%. The reason for this is that a higher flow rate results in an increased amount of liquid phase held in the trickle bed cathode, because of this, the wet film covering the C-PTFE cathode material gets thicker (106). This thicker coating reduces oxygen transport from the gas stage to the electrolyte-cathode interface (108). Moreover, Figure 5.8 demonstrates that an increased electrolyte dosage can also influence the

production of H_2O_2 by affecting the distribution of gas and liquid phases inside the channels of the trickle bed cathode, hence affecting the effectiveness of its removal. Hence, it is important to uphold the ideal electrolyte flow rate in order to effectively eliminate MO in the TBER.

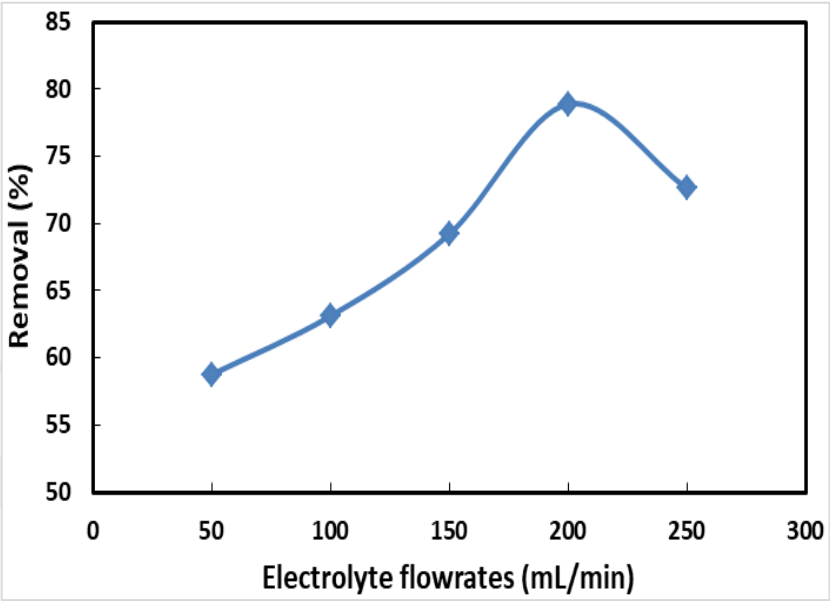

Figure 5.8 MO elimination as a function of the KOH flow rate on methyl orange removal at a potential of 1.0 Volt, 0.2 M electrolyte concentration, 7.0 L/min oxygen flow, 100 ppm methyl orange, and 30°C.

5.1.5 Impact of the Initial concentration.

The elimination rate of MO in modified TBER was studied at various initial concentrations (20, 40, 60, 80, 100) ppm at 1 volt, electrolyte concentration 0.2 M, oxygen flow rate 7 L/min, KOH flow rate 200 mL/min, and reaction temperature 30°C. The results of the experiment are summarised in Appendix 2, Table 8.2. Figure 5.9 depicts the influence of the MO starting concentration on its elimination in TBER.

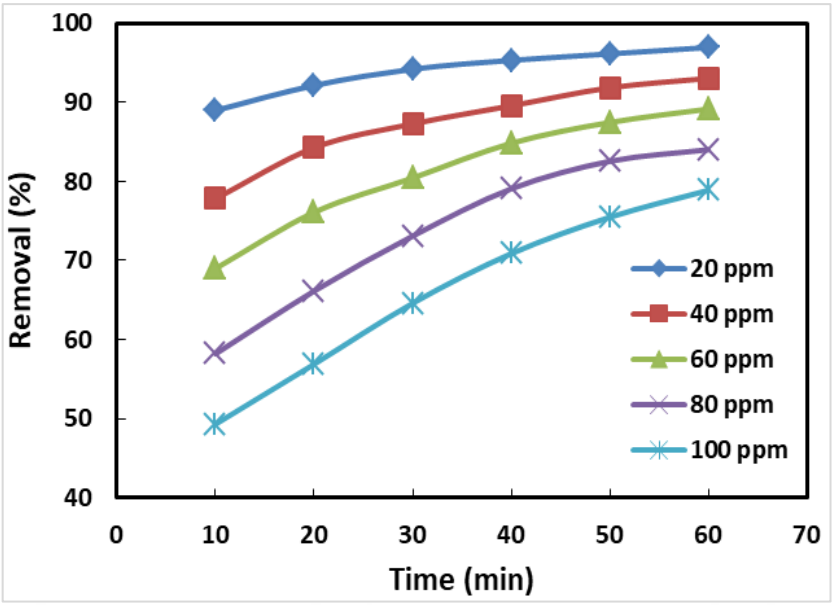

Figure 5.9 Impact of initial concentration of MO (20, 40, 60, 80, and 100 ppm) on the MO concentration plotted against time at 1 V, electrolyte concentration of 0.2M, oxygen flow rate of 7 L/min, electrolyte flow rate of 200 ml/min, and 30°C.

According to the findings, the influence of the initial concentration of MO on elimination efficiency by using TBER was clearly increased from 78.8% to 96.9% when the initial concentration of MO was decreased to 20 ppm from 100 ppm. As a result, there is a negative link between the rate of elimination and the starting concentration of methyl orange. This drop in removal efficiency that was found at higher starting MO concentrations could be attributed to a number of different variables. In the first place, when the concentrations are smaller, a greater proportion of the $OH^{\bullet}$ that is produced during the electrochemical procedure reacts with the MO molecules, which results in a higher elimination efficiency. On the other hand, when the initial concentrations are higher, there is the highest amount of MO molecules present, and the same limited number of $OH^{\bullet}$ are created. This leads to a lower percentage of MO removal. Secondly, when the starting dye concentrations are higher, the pollutant molecules have a propensity to clump together and create aggregates with reduced diffusion coefficients. A slower removal process and less efficiency can result from this agglomeration, slowing the pace at which the dye molecules combine with the hydroxyl radicals (90).

Consequently, the initial concentration of MO significantly influences the removal efficiency of the TBER; higher initial concentrations result in lower removal percentages. As illustrated in Figure 5.10.

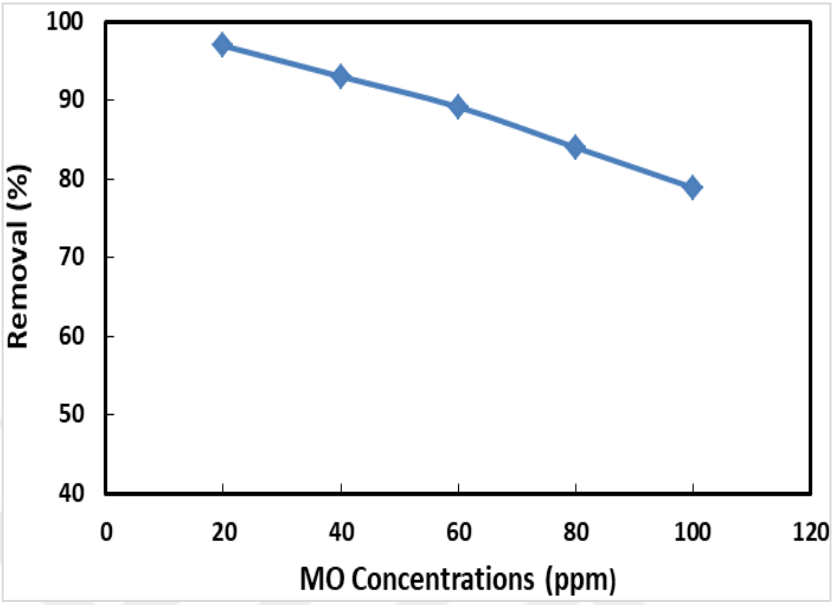

Figure 5.10 The influence of initial methyl orange concentration on methyl orange removal at 30°C, 1.0 V, a 0.2 M electrolyte concentration, a 7 L/min oxygen flow rate , and a 200 ml/min electrolyte flow rate.

5.1.6 Impact of the Reaction Temperature.

An experiment was done to see how temperature affected the rate of MO oxidation in TBER. The experiment used 0.2 M electrolyte concentrations, 200 ml/min electrolyte flow rates, 7 L/min oxygen flow rates, one-volt applied, and 100 ppm methyl orange concentrations. The experiment results are summarised in Appendix 2, Table 8.2.

The elimination effectiveness was studied at different temperatures (5°C, 10°C, 20°C, and 30°C). The studies were conducted using the following operating conditions: A voltage of 1 V was applied, a 0.2 M KOH electrolyte was used, a starting concentration of 100 ppm, and the electrolysis lasted for 60 minutes. The results showed that reaction temperature had an influence on MO reduction effectiveness in the TBER, as illustrated in Figure 5.11.

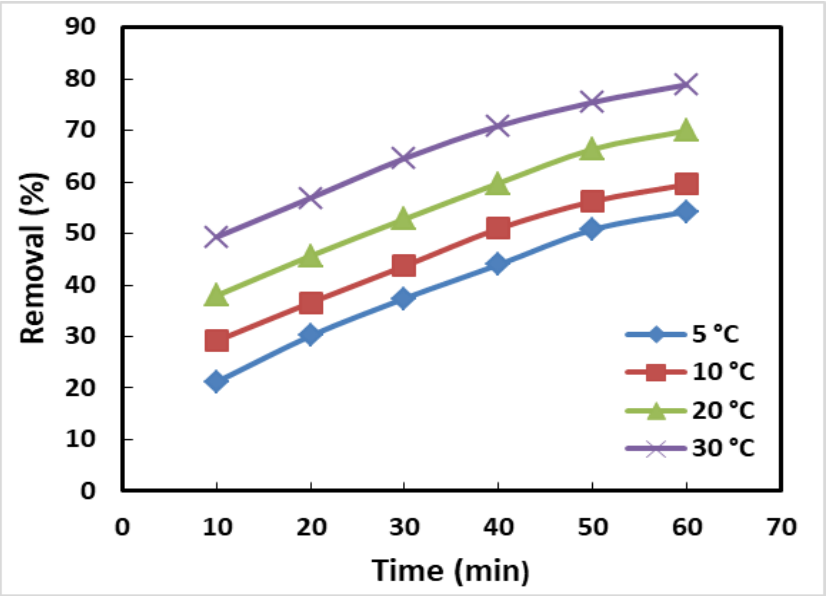

Figure 5.11 The influence of reaction temperature (5, 10, 20, and 30°C) on methyl orange elimination was plotted against time at a voltage of 1 volt, KOH concentration of 0.2 M, oxygen flow rate of 7 L /min, electrolyte flow rate of 200 ml/min, and methyl orange concentration of 100 ppm.

The influence of the reaction temperature on elimination efficiency was studied using TBER. The MO elimination was clerically noticed to rise from 54.2% to 78.8% when the reaction temperature was increased to 30°C from 5°C. The data suggests that the increase in reaction temperature has a positive effect on the elimination of MO. Because, higher temperatures result in greater elimination efficacy for a variety of reasons. To begin with, an increase in temperature leads to a corresponding rise in the generation of H_2O_2, which subsequently facilitates the elimination of MO. Also, rising temperatures may improve MO removal by enhancing the catalytic activity of the C-PTFE catalyst. Increasing the temperature can enhance the efficiency of MO elimination by releasing oxygen during the process.

In general, Figure 5.12 is illustrate. The results of this study indicate that increasing the reaction temperature, specifically up to 30°C in this instance, can greatly enhance the effectiveness of elimination MO in the TBER. Nevertheless, it is important to acknowledge that conducting electrochemical processes at room temperature (about 20°C) is frequently favored due to its lower energy requirement and greater cost-effectiveness, according to previous research (41).

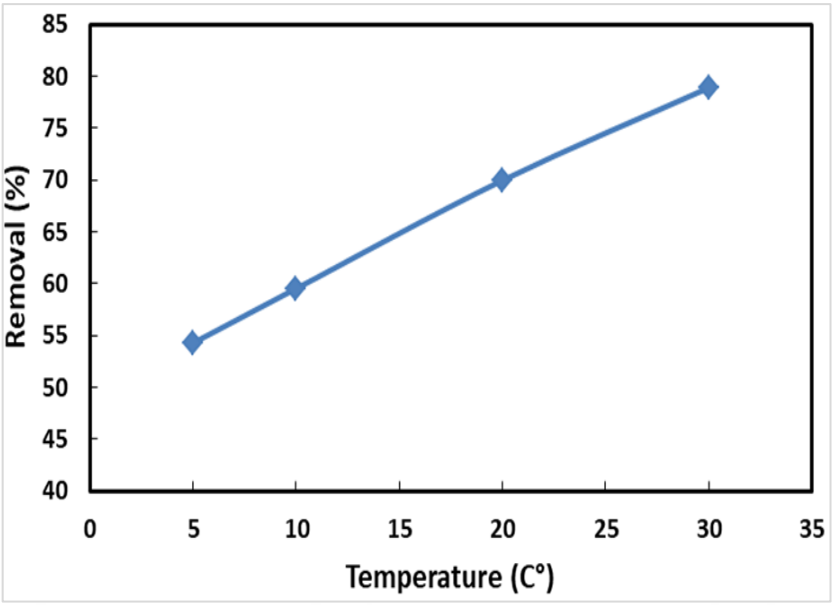

Figure 5.12 The impact of temperature of reaction on methyl orange elimination at 0.2M electrolyte concentration, 200ml/min electrolyte flow rate, 7 L/min oxygen flow rate, one- volt, and 100 ppm MO concentration..

5.1.7 The Effect of Oxygen on MO Removal in the Absence and Presence of Voltage

The experimental results of MO elimination Without Oxygen and With and Without Voltage. Using modified TBER, at an used voltage of 1V, MO concentrations of 100 ppm, oxygen flow rates of 7 L/min, KOH concentrations of 0.2 M, and electrolyte flow rates of 200 ml/min. Table 8.4 in Appendix 2 summarizes the experimental results.

A comparison of the MO elimination efficiency under different operating conditions is shown in Figure 5.13. The evaluation of this comparison was done after determining optimal operating parameters to assess the suggested process's efficiency in eliminating MO compared to other operations, which can be more precisely explained as follows: The cathode layer alone (without any electricity or oxygen). The cathode layer of C-PTFE was utilized in this procedure without the use of electricity or oxygen. The electrolyte flow rate employed in the experiment was 200 ml/min, the concentration of KOH was 0.2 M, and the temperature was 30°C. Only 9.6% of the organic 100 ppm MO was eliminated after 60 minutes, indicating a lack of effectiveness in the absence of oxygen and electricity. However, this suggests that MO can be physically absorbed onto the carbon surface by the cathode layer. Also, this is due to the presence of oxygen atoms on

the C-PTFE layer after acid treatment after every experiment. The second method is electrolytic oxidation (without oxygen, only electricity). No oxygen was added; the experiment was conducted at the same voltage (1 V), duration, and fluid flow rate. After 60 minutes, the effectiveness of the elimination rose to about 27.1%. The enhanced elimination effectiveness is probably due to liquid electrolysis triggered by the applied voltage, resulting in the production of hydroxyl radicals that possess more potent oxidizing properties.

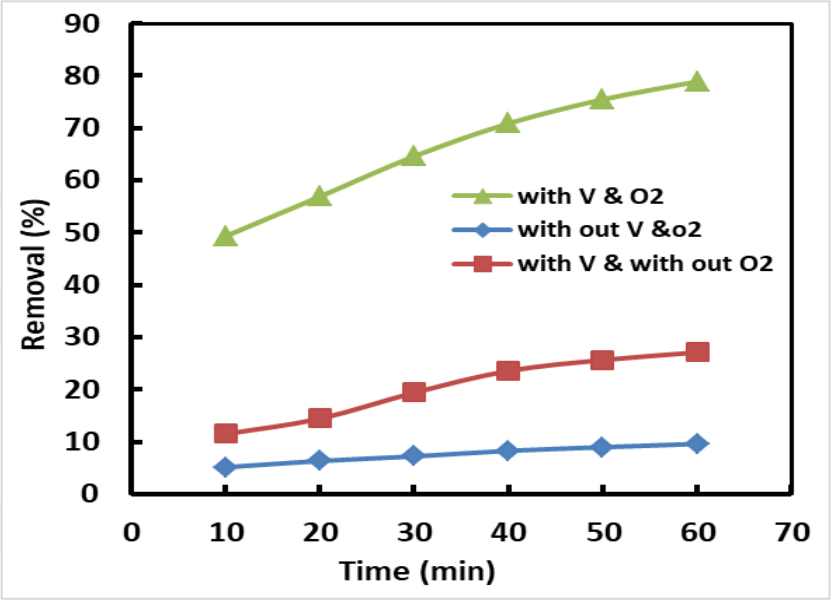

Figure 5.13 In situ oxidation, direct adsorption, eleco-oxidation, and elect-oxidation with and without O_2 flow were utilised to remove methyl orange at 30°C, 0.2 M KOH, 1.0 V, 200 mL/min electrolyte flow rate, 100 ppm MO, and 7.0 L/min O_2 flow rate.

Finally, we carried out the electrolytic oxidation process with oxygen under the same conditions as previously described, but we added the injection of pure O_2 at a flow rate of 7.0 L/min. After a duration of 60 min, the efficiency of MO elimination was 78.9%. The increased rate of clearance can be attributed to the in-situ generation of hydrogen peroxide via the O_2 reduction process (ORR) of oxygen gas (O_2) on the surface of the cathode electrode. The produced hydrogen peroxide generates more hydroxyl radicals, hence increasing the effectiveness of the elimination process. In conclusion, the results show that the suggested approach is highly successful and capable of eliminating organic compounds, even at high concentrations, without the need to add metal ions such as ferric ions, which are considered to be environmental pollutants. Electrolysis, in conjunction

with oxygen injection, greatly enhances the efficacy of MO removal, making this technique a highly promising strategy for wastewater treatment.

5.2 Thermodynamic and Kinetic Study

Adsorption kinetic study is important for giving useful information about the cathode layer surface and adsorb operation during wastewater treatment. The cathode layer is characterized by a high ability to absorb methyl orange dye, especially when its concentration is less than 50 ppm. In our current study, kinetics was calculated by applying the Arrhenius equation to rate constants of the MO in Situ Oxidation at Different Temperatures (5, 10, 20, 30)°C At an applied voltage of 1V, concentrations of electrolyte of 0.2 M, flow rates of electrolyte 200 ml/min, flow rates of oxygen 7 L/min, and concentrations of methyl orange 100 ppm are listed in Appendix 2, Table 8.3, contains a summary of the experimental findings. Figure 5.14 presents the investigation's findings, and you can calculate the reaction rate constants at a range of temperatures using the slopes of the lines. It was discovered that the in-situ oxidation of MO is a first-order process, which is in line with the findings from an earlier study (51,94). Notably, the reaction rate constants rise with increasing oxidation temperature; they range from 0.0111(1/min) at 5°C to 0.0179(1/min) at 30°C. This behaviour, which is temperature-dependent, is consistent with earlier research. However, which found that the dye structure determines the ideal temperatures for removal (41). In general, greater temperatures increase the activity of the catalyst, which simultaneously speeds up the decomposition of the dye and the evolution of oxygen (91).

A calculation was taken of the energy of activation (E) for the MO's in situ oxidizing process. as shown in Figure 5.15. The apparent energy of activation (Ea) was estimated to be 14.0621 kJ/mol by inserting the rate of removal constants recorded between 278.15 K and 303.15 K into the Arrhenius equation. The slope of the line, which is equal to E/R, was utilized to determine this value. The activation energy of TBER MO in situ oxidation suggests that it is a viable technology for effluent reduction. Because the activation energy is positive, the reaction rate grows with rising temperature, indicating the process is rapid and hard to regulate.

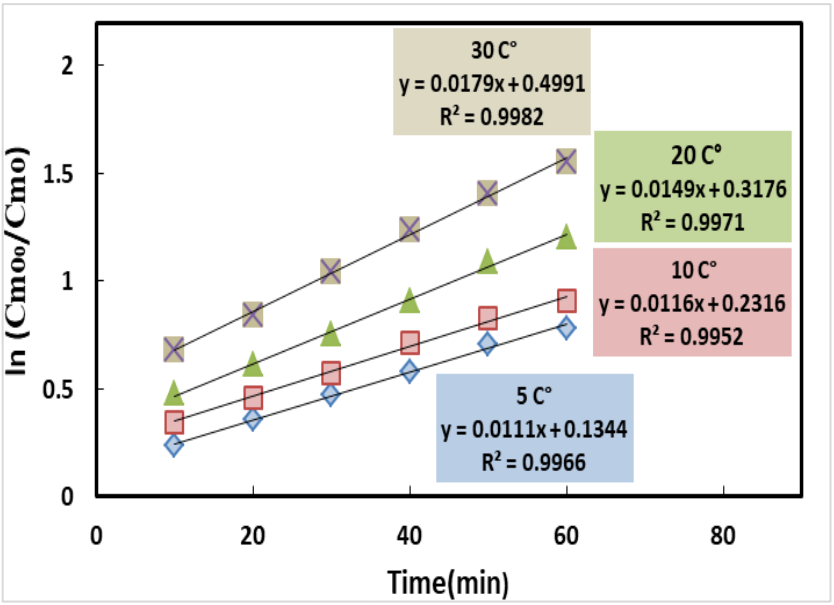

Figure 5.14 The kinetic data was represented by a first-order reaction at temperatures of 5, 10, 20, and 30 °C.

The activation energy serves as a free energy barrier, limiting single-step transitions. Tolman computed the net energy of activation for the full transition time as follows:

$$E_a = E_{TS} - E_R \qquad 5.9$$

where E_{TS} and E_R are the average thermo-dynamical energy and the average energy, respectively, for the initial state. Hence, if E_{TS} is lower than E_R, the net activation value will be negative (101,109).

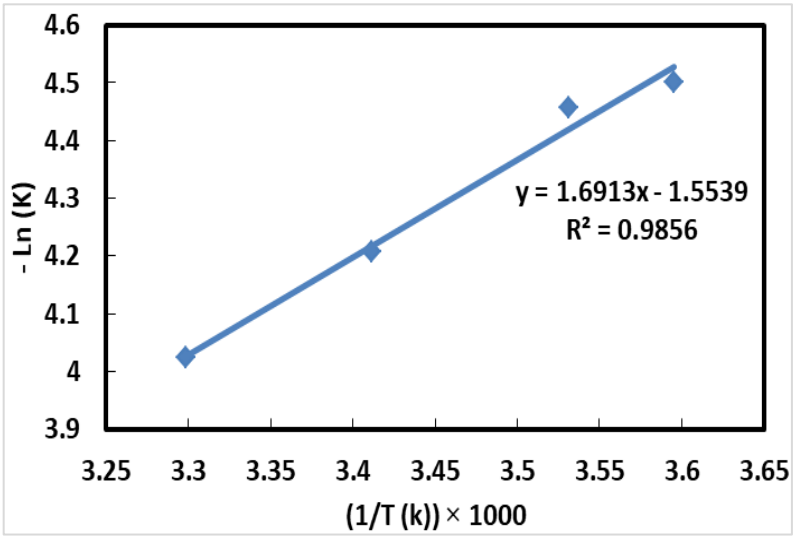

Figure 5.15 At various temperature of 5, 10, 20, and 30°C, an Arrhenius plot is displayed.

Thermodynamic parameters were investigated by using the MO adsorbent on the CB-PTFE adsorbent at temperatures between 278.15 K and 303.15 K. The Van't Hoff graph was used to determine the two thermodynamic variables ΔS° and ΔH° by using a slope and intercept of lnKd vs 1/T as displayed in Figure 5.16. The entropy and enthalpy were found to be 0.1157 KJ/mol k and 31.867 KJ/mol, respectively. In accordance with the ΔS° value (ΔS > 0 for spontaneous operation), the findings are listed in Appendix 2, Table 8.5. The negative data of ΔG° shows that this adsorption operation was spontaneous at temperatures of 278.15, 283.15, 293.15, and 303.15 K. The positive ΔH° values indicated that the adsorption mechanisms were endothermic; the high temperature led to an activated adsorption surface in the system.

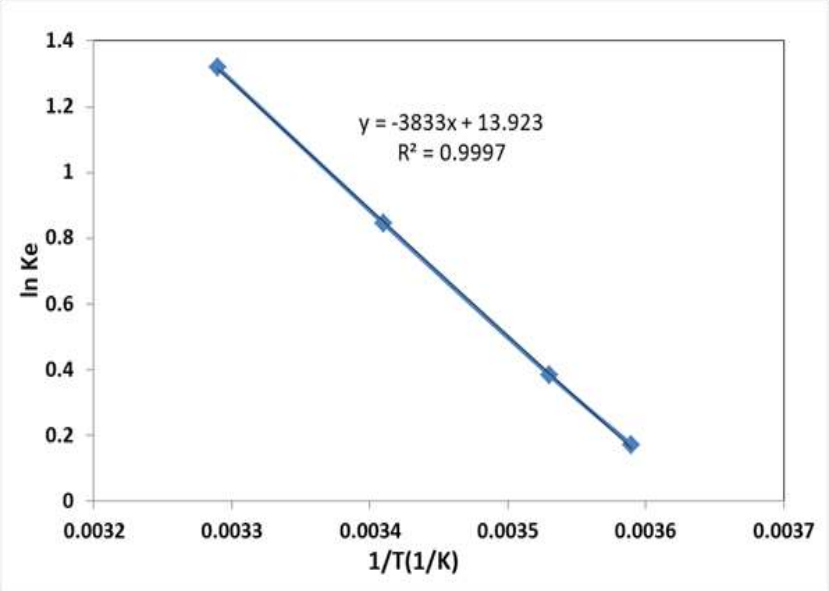

Figure 5.16 Plot ln k_e against 1/T to illustrate how MO is adsorbed on CB-PTFE

5.3 Comparison of the results with the related literature

The results show that the newly created TBER has the right rate of hydrogen peroxide production and endogenous methyl orange oxidation. Specifically in comparison to the findings obtained by other researchers. The amount of methyl orange that can be oxidised to its maximum under ideal conditions is detailed in Table 5.1

Table 5.1 Maximum methyl orange oxidation under optimal conditions.

Cathode material	Anode material	[MO] (ppm)	Removal (%)	Power sapply	Time (hr)	Ref.
Pt	(DTNA) titanium sheet TiO_2	200	85.2	1 mA/cm^2	6	(110)
Pt	Ti/IrO_2	200	31.1	1 mA/cm^2	6	(110)
graphite felt	Ti/Ir-Sn-Sb	30	94	20 mA/cm^2	4-5	(88)
Ti/Pt	Ti/Pt	50	98	4.6 A	1.5	(111)
Al	Pt	50	98	40 mA/cm^2	1	(48)
Ti	PbO_2/Ti	10	53	15 v	0.5	(112)
stainless steel	BDD	50	98	0.5 A	2	(82)
GDE (CB-PTFE)	Stainless Steel	100	78.8	1 V	1	Present study

6. CONCLUSIONS

The following outcomes were concluded significantly from the results of the current thesis study:

1. The maximum electrochemical oxidation-based MO removals of 96.9%, 93%, and 78.8% were obtained under the operating conditions of 1 V, electrolyte concentration of 0.2 M, electrolyte flow rate of 200 ml/min, oxygen flow rate of 7 L/min, temperature 30°C for initial MO concentrations of 20, 40, and 100 ppm, respectively.
2. Increasing the applied voltage, electrolyte flow rate and oxygen flow rate led to an increase in electrochemical oxidation-based MO elimination, whereas an increase in the initial MO concentration and electrolyte concentration decreased the efficiency. Moreover, increasing the same factors over a specific limit led to a certain decrease in removal efficiency. Additionally positive effect of temperature was observed as a driving force which led to an increase in elimination efficiency.
3. Kinetics studies showed that the degradation of MO by TBER process fitted well with pseudo-first-order kinetics. Reaction rate constants were determined as 0.0111 (1/min) and 0.0179 (1/min) at 5°C and 30°C, respectively. Depending on these findings, activation energy was estimated as 14.0621 kJ/mol.
4. According to the findings, it can be concluded that TBER contributed to related literature significantly. Its eco-friendly way may be evaluated as a promising process in terms of less need for chemicals.

Given the hypotheses which had been put forward and motivations which had been determined to test the hypotheses, it can be clearly seen that all the hypotheses were justified. Good accordance between the results of the present study and the related literature demonstrated the accuracy of the present thesis study significantly.

6.1 Suggestions for future projects

The following suggestions may contribute to filling the gap in related literature.

1. Examining the impact of different layers of catalyst on the efficacy of electrochemical oxidation process may contribute to related literature.
2. Utilization of graphite for both anode and cathode may also contribute to increase the removal efficiency.
3. Various metal oxides such as SiO_2, ZnO, MgO_2 can be investigated to improve the electrogeneration of hydrogen peroxide.
4. Acidic medium conditions may be used instead of employing an alkaline solution to decrease the operational cost.
5. Various model dyes, dyestuff, and pigments may be used instead of MO.
6. In future studies, statistics-based approaches may be utilized for the design of experiments and some useful models may be derived to descend the error probability, decrease the operational cost, and lower the number of the sets of experiments.

7. REFERENCES

"Vancouver citation system was used in this thesis."

1. Yadav S, Dhir MA. Decolourization of Dye & Textile Effluent using Advanced Oxidation Processes Under the Supervision of. 2008.

2. Haiming ZOU, Zhili SUN, Jiao Z, Wang Y. AZO DYE WASTEWATER TREATMENT in A NOVEL THREE-DIMENSIONAL ELECTRODE REACTOR. Environ Prot Eng. 2022;48(2):5–13.

3. Lellis B, Fávaro-polonio CZ, Pamphile JA, Polonio JC. Effects of textile dyes on health and the environment and bioremediation potential of living organisms. 2019;

4. Xu L, Zhao H, Shi S, Zhang G, Ni J. Electrolytic treatment of C.I. Acid Orange 7 in aqueous solution using a three-dimensional electrode reactor. Dye Pigment. 2008;77(1):158–64.

5. Restiani P. Water Governance Mapping Report : Textile Industry Water Use In India Focus On The Faridabad-Ballabgarh Textile Cluster In The State Of Haryana. Sustain Outlook. 2016;1–56.

6. Bhatia D, Sharma NR, Singh J, Kanwar RS. Biological methods for textile dye removal from wastewater: A review. Crit Rev Environ Sci Technol. 2017;47(19):1836–76.

7. Pereira L, Alves M. Dyes-environmental impact and remediation. Environ Prot Strateg Sustain Dev. 2012;111–62.

8. Rodríguez M. Fenton and UV-vis based advanced oxidation processes in wastewater treatment: Degradation, mineralization and biodegradability enhancement. Dep D'Enginyeria Quim I Met [Internet]. 2003;296. Available from: http://diposit.ub.edu/dspace/handle/2445/35398

9. Al-Kdasi A, Idris A, Saed K, Guan CT. Treatment of textile wastewater by advanced oxidation processes– A review. Glob Nest J. 2004;6(1):222–30.

10. Hussain S, Khan N, Gul S, Khan S, Khan H. Contamination of Water Resources by Food Dyes and Its Removal Technologies. Water Chem. 2020;

11. Editor T, Access O, Commons C, Licence ACD, By-nc-nd CC. Photocatalytic Water and Wastewater Treatment. Photocatalytic Water and Wastewater Treatment. 2022.

12. Punzi M. Treatment of textile wastewater by combining biological processes and advanced oxidation. [Internet]. Department of Biotechnology, Lund University; 2015. Available from: lund: Department of Biotechnology, Lund University,

13. Sujata Mani, Pankaj Chowdhary and RNB. Textile Wastewater Dyes: Toxicity Profile and Treatment Approaches. Springer Nat Singapore Pte Ltd. 2019;219.

14. Sirés I, Brillas E, Oturan MA, Rodrigo MA, Panizza M. Electrochemical advanced oxidation processes: Today and tomorrow. A review. Environ Sci Pollut Res. 2014;21(14):8336–67.

15. Pandis PK, Kalogirou C, Kanellou E, Vaitsis C, Savvidou MG, Sourkouni G, et al. Key Points of Advanced Oxidation Processes (AOPs) for Wastewater, Organic Pollutants and Pharmaceutical Waste Treatment: A Mini Review. ChemEngineering. 2022;6(1).

16. Collins J and BJR. Advanced Oxidation Handbook. Am Water Work Assoc. 2016;

17. Singh K, Arora S. Removal of synthetic textile dyes from wastewaters: A critical review on present treatment technologies. Crit Rev Environ Sci Technol. 2011;41(9):807–78.

18. Deng Y, Zhao R. Advanced Oxidation Processes (AOPs) in Wastewater Treatment. Curr Pollut Reports. 2015;1(3):167–76.

19. Nidheesh P V., Zhou M, Oturan MA. An overview on the removal of synthetic dyes from water by electrochemical advanced oxidation processes. Chemosphere. 2018;197:210–27.

20. Chen G, Hung Y. Electrochemical Wastewater Treatment Processes. 2007;5.

21. ELECTROCHEMICAL TREATMENT OF TEXTILE DYE WASTEWATER BY ALUMINIUM AND STAINLESS-STEEL ELECTRODES. 2020;

22. Kaur A. Investigation of azo-bond cleavage in Methyl Orange and Direct Yellow 12 using soybean peroxidase. 2020;

23. Editors AM• EG• RA. Environmental Deterioration and Human Health. 2014.

24. Vijaykumar MH, Vaishampayan PA, Shouche YS, Karegoudar TB. Decolourization of naphthalene-containing sulfonated azo dyes by Kerstersia sp. strain VKY1. Enzyme Microb Technol. 2007;40(2):204–11.

25. Vautier M, Guillard C, Herrmann JM. Photocatalytic degradation of dyes in water: Case study of indigo and of indigo carmine. J Catal. 2001;201(1):46–59.

26. Brezová V, Pigošová J, Havlínová B, Dvoranová D, Ďurovič M. EPR study of photochemical transformations of triarylmethane dyes. Dye Pigment. 2004;61(2):177–98.

27. Yellow A, Brown M, Brown B. 3 The chemistry of azo dyes H , N-O-N ~ N-O-N ~ N-b-NH ’. 1971;21–2.

28. Wu L, Liu X, Lv G, Zhu R, Tian L, Liu M, et al. Study on the adsorption properties of methyl orange by natural one-dimensional nano-mineral materials with different structures. Sci Rep [Internet]. 2021;11(1):1–11. Available from: https://doi.org/10.1038/s41598-021-90235-1

29. Guettaı N, Amar HA. Photocatalytic oxidation of methyl orange in presence of titanium dioxide in aqueous suspension . Part I : Parametric study. 2005;185(May):427–37.

30. Lin H, Lin H. Removal of organic pollutants from water by electro-Fenton and electro-Fenton like processes To cite this version : HAL Id : tel-01336262. 2016;

31. Brillas E, Martínez-Huitle CA. Decontamination of wastewaters containing synthetic organic dyes by electrochemical methods. An updated review. Appl Catal B Environ. 2015;166–167:603–43.

32. Vijayaraghavan J, Sardhar Basha SJ, Jegan J. A review on efficacious methods to decolorize reactive azo dye. J Urban Environ Eng. 2013;7(1):30–47.

33. Razo-Flores E, Luijten M, Donlon B, Lettinga G, Field J. Biodegradation of selected azo dyes under methanogenic conditions. Water Sci Technol. 1997;36(6–7):65–72.

34. Habibi MH, Talebian N. Photocatalytic degradation of an azo dye X6G in water : A comparative study using nanostructured indium tin oxide and titanium oxide thin films. 2007;73:186–94.

35. Awad HS, Galwa NA. Electrochemical degradation of Acid Blue and Basic Brown dyes on Pb/PbO2 electrode in the presence of different conductive electrolyte and effect of various operating factors. Chemosphere. 2005;61(9):1327–35.

36. Zhou M, Särkkä H, Sillanpää M. A comparative experimental study on methyl orange degradation by electrochemical oxidation on BDD and MMO electrodes. Sep Purif Technol [Internet]. 2011;78(3):290–7. Available from: http://dx.doi.org/10.1016/j.seppur.2011.02.013

37. Dinkar Gosavi V, Sharma S. A general review on various treatment methods for textile wastewater. J Environ Sci Comput Sci Eng Technol 3 29-39 [Internet]. 2013;3(1):29–39. Available from: www.jecet.org

38. Long Y, Li H, Xing X, Ni J. Enhanced removal of Microcystis aeruginosa in BDD-CF electrochemical system by simple addition of Fe2+. Chem Eng J [Internet]. 2017;325:360–8. Available from: http://dx.doi.org/10.1016/j.cej.2017.05.067

39. Lahkimi A, Oturan MA, Oturan N, Chaouch M. Removal of textile dyes from water by the electro-Fenton process. Environ Chem Lett. 2007;5(1):35–9.

40. Meas-vong Y, Rodrı FJ, Chapman TW, Maldonado MI, Godı LA. Comparison of hydrogen peroxide-based processes for treating dye-containing wastewater : Decolorization and destruction of Orange II azo dye in dilute solution. 2008;76:656–62.

41. Martínez-Huitle CA, Rodrigo MA, Sirés I, Scialdone O. Single and Coupled Electrochemical Processes and Reactors for the Abatement of Organic Water Pollutants: A Critical Review. Chem Rev. 2015;115(24):13362–407.

42. Jasim BI. An Advanced Oxidation Process of Tetracycline in Waste Water Using A double Layer Cathode Reactor. Surv Fish Sci. 2023;

43. Faouzi AM, Nasr B, Abdellatif G. Electrochemical degradation of anthraquinone dye Alizarin Red S by anodic oxidation on boron-doped diamond. Dye Pigment. 2007;73(1):86–9.

44. Zhao G, Gao J, Shi W, Liu M, Li D. Electrochemical incineration of high concentration azo dye wastewater on the in situ activated platinum electrode with sustained microwave radiation. Chemosphere [Internet]. 2009;77(2):188–93. Available from: http://dx.doi.org/10.1016/j.chemosphere.2009.07.044

45. Tyagi VK, Ojha CSP. Landfill leachate management. Landfill Leachate Management. 2023. 1–467 p.

46. Yi S, Ma Y, Wang X, Jia Y. Green chemistry : Pretreatment of seawater by a one-step electrochemical method. DES [Internet]. 2009;239(1–3):247–56. Available from: http://dx.doi.org/10.1016/j.desal.2008.03.021

47. Ammar HB, Brahim M Ben, Abdelhédi R, Samet Y. Green electrochemical process for metronidazole degradation at BDD anode in aqueous solutions via direct and indirect oxidation. Sep Purif Technol [Internet]. 2016;157:9–16. Available from: http://dx.doi.org/10.1016/j.seppur.2015.11.027

48. Rao ANS, Venkatarangaiah VT. The effect of cathode materials on indirect electrochemical oxidation of methyl orange, malachite green and methylene blue. Port Electrochim Acta. 2014;32(3):213–31.

49. Santos D, Lopes A, Pacheco MJ, Gomes A, Cir L. The Oxygen Evolution Reaction at Sn-Sb Oxide Anodes : Influence of the Oxide Preparation Mode The Oxygen Evolution Reaction at Sn-Sb Oxide Anodes : Influence. 2014;(November 2015).

50. Labiadh L, Barbucci A, Carpanese MP, Gadri A, Ammar S, Panizza M. Direct and indirect electrochemical oxidation of Indigo Carmine. 2017;(August).

51. Wang G, Liu Y, Ye J, Lin Z, Yang X. Electrochemical oxidation of methyl orange by a Magnéli phase Ti4O7 anode. ECSN [Internet]. 2019;125084. Available from: https://doi.org/10.1016/j.chemosphere.2019.125084

52. Zhang X, Shao D, Lyu W, Tan G, Ren H. Utilizing discarded SiC heating rod to fabricate SiC / Sb-SnO 2 anode for electrochemical oxidation of wastewater. Chem Eng J [Internet]. 2018; Available from: https://doi.org/10.1016/j.cej.2018.12.085

53. Abdel-Aziz MH, Bassyouni M, Zoromba MS, Alshehri AA. Removal of Dyes from Waste Solutions by Anodic Oxidation on an Array of Horizontal Graphite Rods Anodes. Ind Eng Chem Res. 2019;58(2):1004–18.

54. Urtiaga A, Ortiz I. Contributions of electrochemical oxidation to waste-water treatment : fundamentals. 2009;(March):1747–55.

55. Barros WRP, Franco PC, Steter JR, Rocha RS, Lanza MR V. Author ' s personal copy Electro-Fenton degradation of the food dye amaranth using a gas diffusion electrode modified with cobalt (II) phthalocyanine.

56. Chemically modified graphite felt as an efficient cathode in electro-Fenton for p-nitrophenol degradation. 2014;

57. Luo H, Li C, Wu C, Zheng W, Dong X. Electrochimica Acta Electrochemical degradation of phenol by in situ electro-generated and electro-activated hydrogen peroxide using an improved gas diffusion cathode. Electrochim Acta [Internet]. 2015;186:486–93. Available from: http://dx.doi.org/10.1016/j.electacta.2015.10.194

58. Hamdan HY, Abdullah GH. Chemical Engineering and Processing - Process Intensification A novel trickle bed electrochemical reactor design for efficient hydrogen peroxide production. Chem Eng Process - Process Intensif [Internet]. 2022;181(May):109123. Available from: https://doi.org/10.1016/j.cep.2022.109123

59. Özcan A, Şahin Y, Savaş Koparal A, Oturan MA. Carbon sponge as a new cathode material for the electro-Fenton process: Comparison with carbon felt cathode and application to degradation of synthetic dye basic blue 3 in aqueous medium. J Electroanal Chem. 2008;616(1–2):71–8.

60. Martínez-Huitle CA, Brillas E. Decontamination of wastewaters containing synthetic organic dyes by electrochemical methods: A general review. Appl Catal B Environ. 2009;87(3–4):105–45.

61. Yong K, Zhi-liang W, Yu W, Jia Y, Zhi-dong C. Degradation of methyl orange in artificial wastewater through electrochemical oxidation using exfoliated graph- ite electrode. New Carbon Mater [Internet]. 2011;26(6):459–64. Available from: http://dx.doi.org/10.1016/S1872-5805(11)60092-9

62. Popli SA, Patel UD. Electrochemical decolourization of reactive black 5 in an undivided cell using ti and graphite anodes: Effect of polypyrrole coating on anodes. J Electrochem Sci Eng. 2015;5(2):145–56.

63. Bar MD, Morales-ortiz U, Sort J, Brillas E. Comparative electrochemical oxidation of methyl orange azo dye using Ti / Ir-Pb , Ti / Ir-Sn , Ti / Ru-Pb , Ti / Pt-Pd and Ti / RuO 2. Electrochim Acta [Internet]. 2017; Available from: http://dx.doi.org/10.1016/j.electacta.2017.05.101

64. Koparal AS, Yavuz Y, Gürel C, Öğütveren ÜB. Electrochemical degradation and toxicity reduction of C.I. Basic Red 29 solution and textile wastewater by using diamond anode. J Hazard Mater. 2007;145(1–2):100–8.

65. El-Ghenymy A, Centellas F, Garrido JA, Rodríguez RM, Sirés I, Cabot PL, et al. Decolorization and mineralization of Orange G azo dye solutions by anodic oxidation with a boron-doped diamond anode in divided and undivided tank reactors. Electrochim Acta [Internet]. 2014;130:568–76. Available from: http://dx.doi.org/10.1016/j.electacta.2014.03.066

66. Saldan A, Acero R, Guerra R, Herna B, Ramı C, Garcia-segura S, et al. Journal of Industrial and Engineering Chemistry Electrochemical oxidation of methyl orange azo dye at pilot flow plant using BDD technology. 2013;19:571–9.

67. Do MH, Phan NH, Nguyen TD, Pham TTS, Nguyen VK, Vu TTT, et al. Activated

carbon/Fe3O4 nanoparticle composite: Fabrication, methyl orange removal and regeneration by hydrogen peroxide. Chemosphere [Internet]. 2011;85(8):1269–76. Available from: http://dx.doi.org/10.1016/j.chemosphere.2011.07.023

68. Schwidder S, Schnitzlein K. A new model for the design and analysis of trickle bed reactors. Chem Eng J [Internet]. 2012;207–208:758–65. Available from: http://dx.doi.org/10.1016/j.cej.2012.07.054

69. Lei Y, Liu H, Shen Z, Wang W. Development of a trickle bed reactor of electro-Fenton process for wastewater treatment. J Hazard Mater [Internet]. 2013;261:570–6. Available from: http://dx.doi.org/10.1016/j.jhazmat.2013.08.010

70. Brillas E, Sirés I, Oturan MA, Cardoso IMF, Cardoso RMF, Esteves da Silva JCG, et al. Electro-Fenton Process and Related Electrochemical Technologies Based on Fenton's Reaction Chemistry. Curr Pollut Reports [Internet]. 2009;1(12):6570–631. Available from: https://doi.org/10.1016/j.chemosphere.2020.129225%0Ahttps://doi.org/10.1080/01496395.2018.1512618%0Ahttps://doi.org/10.1007/s10653-022-01326-5

71. Garcia-Segura S, Keller J, Brillas E, Radjenovic J. Removal of organic contaminants from secondary effluent by anodic oxidation with a boron-doped diamond anode as tertiary treatment. J Hazard Mater [Internet]. 2015;283:551–7. Available from: http://dx.doi.org/10.1016/j.jhazmat.2014.10.003

72. Hamza M, Abdelhedi R, Brillas E, Sirés I. Comparative electrochemical degradation of the triphenylmethane dye Methyl Violet with boron-doped diamond and Pt anodes. J Electroanal Chem [Internet]. 2009;627(1–2):41–50. Available from: http://dx.doi.org/10.1016/j.jelechem.2008.12.017

73. Mittal A, Malviya A, Kaur D, Mittal J, Kurup L. Studies on the adsorption kinetics and isotherms for the removal and recovery of Methyl Orange from wastewaters using waste materials. J Hazard Mater. 2007;148(1–2):229–40.

74. Qiao Q, Singh S, Lo S, Li Y, Jin J, Wang L. Journal of the Taiwan Institute of Chemical Engineers Electrochemical oxidation of acid orange 7 dye with Ce , Nd , and Co-modified PbO 2 electrodes : Preparation , characterization , optimization , and mineralization. 2018;84:110–22.

75. Chen J, Xia Y, Dai Q. Electrochemical degradation of chloramphenicol with a novel Al doped PbO 2 electrode : Performance , kinetics and degradation mechanism. Elsevier Ltd [Internet]. 2015; Available from: http://dx.doi.org/10.1016/j.electacta.2015.02.029

76. Xu X, Chen J, Zhang G, Song Y, Yang F. Homogeneous Electro-Fenton Oxidative Degradation of Reactive Brilliant Blue Using a Graphene Doped Gas-Diffusion Cathode. 2014;9:569–79.

77. Treatment EW, Ba JA, El-ghenymy A, Rodríguez FJ, Manríquez J, Bustos E. Study of an Air Diffusion Activated Carbon Packed Electrode for an. 2014;

78. Yu H, Li Y, Zhao M, Dong H, Yu H, Zhan S, et al. Energy-saving removal of methyl orange in high salinity wastewater by electrochemical oxidation via a novel Ti/SnO2-Sb anode—Air diffusion cathode system. 2015;2–7.

79. Wessling DM. Tubular carbon nanotube-based gas diffusion electrode removes persistent organic pollutants by a cyclic adsorption - electro-Fenton process. J Hazard Mater [Internet]. 2015; Available from: http://dx.doi.org/10.1016/j.jhazmat.2015.12.066

80. Thiam A, Sirés I, Garrido JA, Rodríguez RM, Brillas E. Decolorization and mineralization of Allura Red AC aqueous solutions by electrochemical advanced oxidation processes. J Hazard Mater. 2015 Jun 5;290:34–42.

81. Lei Y, Liu H, Jiang C, Shen Z, Wang W. A Trickle Bed Electrochemical Reactor for Generation of Hydrogen Peroxide and Degradation of an Azo Dye in Water.

2015;18(1):47–56.

82. Labiadh L, Barbucci A, Carpanese MP, Gadri A, Ammar S, Panizza M. Comparative depollution of Methyl Orange aqueous solutions by electrochemical incineration using TiRuSnO2, BDD and PbO2 as high oxidation power anodes. J Electroanal Chem [Internet]. 2016;766:94–9. Available from: http://dx.doi.org/10.1016/j.jelechem.2016.01.036

83. Liang L, An Y, Zhou M, Yu F, Liu M. Journal of Environmental Chemical Engineering Novel rolling-made gas-diffusion electrode loading trace transition metal for ef fi cient heterogeneous electro-Fenton-like. Biochem Pharmacol [Internet]. 2016;4(4):4400–8. Available from: http://dx.doi.org/10.1016/j.jece.2016.10.006

84. Yang C. Decoloration of azo dye methyl orange by a novel electro-Fenton internal circulation batch reactor. 2017;(1):1–9.

85. Li K, Liu J, Li J, Wan Z. Effects of N mono- and N/P dual-doping on H2O2, ·OH generation, and MB electrochemical degradation efficiency of activated carbon fiber electrodes [Internet]. ECSN. Elsevier Ltd; 2017. Available from: https://doi.org/10.1016/j.chemosphere.2017.11.111

86. M. K DK, kumarT.M DM, R. M DM, guru K. "Decolourisation of Synthetic and Textile Wastewater by Fenton Process." IOSR J Environ Sci Toxicol Food Technol. 2017;11(03):16–24.

87. Jin T, Wan J, Dai C, Qu S, Shao J, Ma F. A simple method to prepare high specific surface area reed straw activated carbon cathodes for in situ generation of H2O2 and ·OH for phenol degradation in wastewater. J Appl Electrochem [Internet]. 2018;48(3):343–53. Available from: http://dx.doi.org/10.1007/s10800-018-1162-x

88. Márquez AA, Sirés I, Brillas E, Nava JL. Mineralization of Methyl Orange azo dye by processes based on H2O2 electrogeneration at a 3D-like air-diffusion cathode. Chemosphere [Internet]. 2020;259:127466. Available from: https://doi.org/10.1016/j.chemosphere.2020.127466

89. Geraldino HCL, Freitas TKFS, Manholer DD, França F, Oliveira JH, Volnistem EA, et al. Electrochemical generation of H2O2 using gas diffusion electrode improved with rGO intensified with the Fe3O4/GO catalyst for degradation of textile wastewater. J Water Process Eng. 2020;36(May).

90. Elbatea AA, Nosier SA, Zatout AA, Hassan I, Sedahmed GH, Abdel-Aziz MH, et al. Removal of reactive red 195 from dyeing wastewater using electro-Fenton process in a cell with oxygen sparged fixed bed electrodes. J Water Process Eng [Internet]. 2021;41(March):102042. Available from: https://doi.org/10.1016/j.jwpe.2021.102042

91. Pang L, Wang H, Bian ZY. Treatment of methyl orange dye wastewater by cooperative electrochemical oxidation in anodic-cathodic compartment. Water Sci Technol. 2013;67(3):521–6.

92. Daneshvar N, Aber S, Vatanpour V, Rasoulifard MH. Electro-Fenton treatment of dye solution containing Orange II: Influence of operational parameters. J Electroanal Chem. 2008;615(2):165–74.

93. Song S, Fan J, He Z, Zhan L, Liu Z, Chen J, et al. Electrochemical degradation of azo dye C.I. Reactive Red 195 by anodic oxidation on Ti/SnO2-Sb/PbO2 electrodes. Electrochim Acta. 2010;55(11):3606–13.

94. Huimin Yang, Jintao Liang, Li Zhang ZL. Electrochemical Oxidation Degradation of Methyl Orange Wastewater by Nb / PbO 2 Electrode. Int J Electrochem Sci. 2016;Volume 11,(2):1121–34.

95. Yildirim OA. 2022 DETRIMENTAL EFFECTS OF COMMONLY USED TEXTILE

DYES ON THE AQUATIC ENVIRONMENT AND HUMAN HEALTH – A REVIEW. 2022;(October).

96. Abdulla GH. In situ diesel desulfurization in divided-cell trickle bed electrochemical reactor. 2017;

97. Qiang Z, Chang J, Huang C. Electrochemical generation of hydrogen peroxide from dissolved oxygen in acidic solutions. 2002;36:85–94.

98. Agladze GR, Tsurtsumia GS, Jung BI, Kim JS, Gorelishvili G. Comparative study of hydrogen peroxide electro-generation on gas-diffusion electrodes in undivided and membrane cells. J Appl Electrochem. 2007;37(3):375–83.

99. Oloman C, Watkinson AP. Hydrogen peroxide production in trickle-bed electrochemical reactors. J Appl Electrochem. 1979;9(1):117–23.

100. Brillas E, Bastida RM, Llosa E, Casado J. TECHNICAL PAPERS ELECTROCHEMICAL SCIENCE AND TECHNOLOGY Electrochemical Destruction of Aniline and 4-Chloroaniline for Wastewater Treatment Using a Carbon-PTFE 02-Fed Cathode Ph bO lq I. Electrochem Sci Technol. 1995;142(6):1733–41.

101. Yousif SH, Abdullah GH. Development of a New Process for Phenol In Situ Oxidation Using a Bifunctional Cathode Reactor. 2023;

102. GUPTA N. SCALE-UP OF THE PERFORATED BIPOLE TRICKLE BED ELECTROCHEMICAL REACTOR FOR THE GENERATION OF ALKALINE PEROXIDE. 2004;(March).

103. Carmo M, Linardi M, Poco JGR. Characterization of nitric acid functionalized carbon black and its evaluation as electrocatalyst support for direct methanol fuel cell applications. Appl Catal A Gen. 2009;355(1–2):132–8.

104. Paz EC, Aveiro LR, Pinheiro VS, Souza FM, Lima VB, Silva FL, et al. Evaluation of H2O2 electrogeneration and decolorization of Orange II azo dye using tungsten oxide nanoparticle-modified carbon. Appl Catal B Environ. 2018 Sep 15;232:436–45.

105. Pang T, Wang Y, Yang H, Wang T, Cai W. Dynamic model of organic pollutant degradation in three dimensional packed bed electrode reactor. Chemosphere [Internet]. 2018;206:107–14. Available from: https://doi.org/10.1016/j.chemosphere.2018.04.118

106. Abdullah GH, Xing Y. Hydrogen peroxide generation in divided-cell trickle bed electrochemical reactor. Ind Eng Chem Res. 2017;56(39):11058–64.

107. DA COSTA MOREIRA MF. Electrochemical Advanced Oxidation processes:Application to the Degradation of Synthetic and Real Wastewater. 2016;

108. Lei Y, Liu H, Jiang C, Shen Z, Wang W. A trickle bed electrochemical reactor for generation of hydrogen peroxide and degradation of an azo dye in water. J Adv Oxid Technol. 2015;18(1):47–56.

109. Bhunia A, Bansal K, Henini M, Alshammari MS, Datta S. Negative activation energy and dielectric signatures of excitons and excitonic Mott transitions in quantum confined laser structures. J Appl Phys. 2016;120(14).

110. Mo C, Wei H, Wang T. Fabrication of a self-doped TiO2 nanotube array electrode for electrochemical degradation of methyl orange. J Chinese Chem Soc. 2019;66(7):740–7.

111. Oukili K, Loukili M. Optimization of textile azo dye degradation by electrochemical oxidation using Box-Behnken design. Mediterr J Chem. 2019;8(5):410–9.

112. Tian J, Shang K, Xue X, Yang L. Degradation of methyl orange waste water by electrochemical oxidation method. J Phys Conf Ser. 2013;418(1):2–7.

8. APPENDICES

8.1 Appendix 1

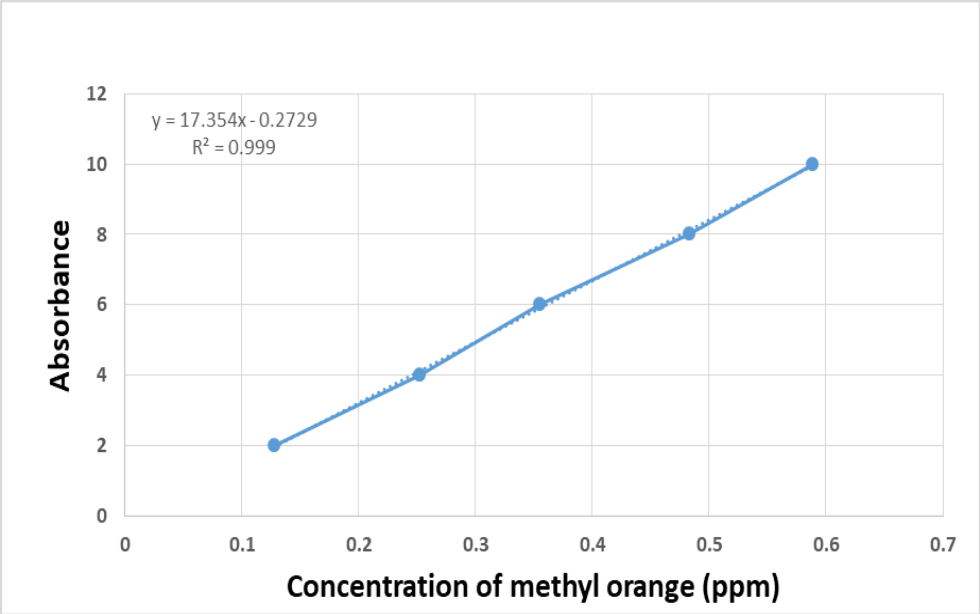

Figure 8.1 Calibration Curves of Methyl orange from 2 to 10 ppm.

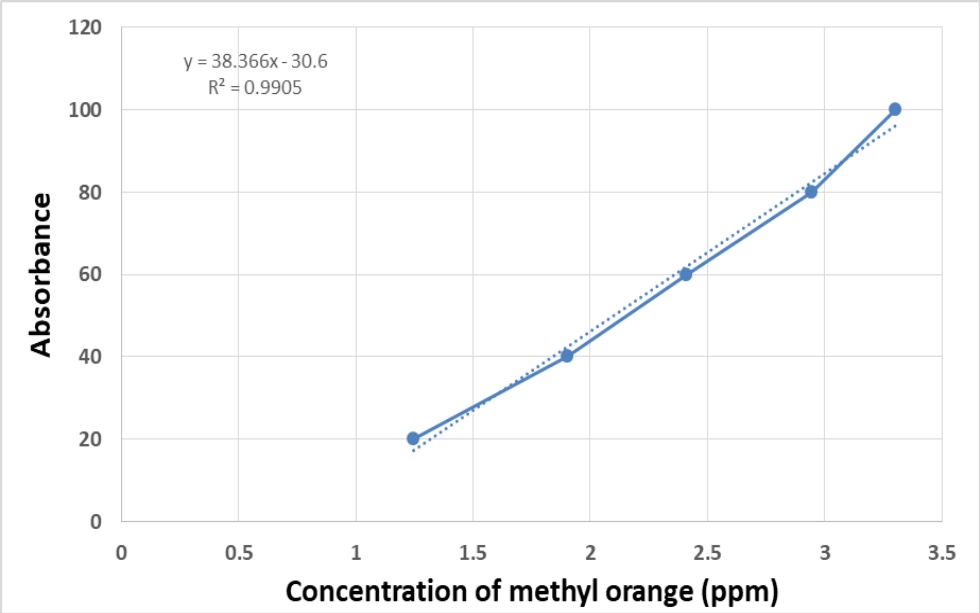

Figure 8.2 Calibration Curves of Methyl orange from 20 to 100 ppm.

8.2 Appendix 2. Tables of Experiments and Results

Table 8.1 Experimental schedule for removal of MO using TBER.

Run	T (min)	Volt (V)	[KOH] (M)	FR1 (ml/min)	FR2 (L/min)	[MO] (ppm)	Temp (°C)
1	10	0.5	0.4	200	3	10	30
2	20	0.5	0.4	200	3	10	30
3	30	0.5	0.4	200	3	10	30
4	40	0.5	0.4	200	3	10	30
5	50	0.5	0.4	200	3	10	30
6	60	0.5	0.4	200	3	10	30
7	10	1	0.4	200	3	10	30
8	20	1	0.4	200	3	10	30
9	30	1	0.4	200	3	10	30
10	40	1	0.4	200	3	10	30
11	50	1	0.4	200	3	10	30
12	60	1	0.4	200	3	10	30
13	10	2	0.4	200	3	10	30
14	20	2	0.4	200	3	10	30
15	30	2	0.4	200	3	10	30
16	40	2	0.4	200	3	10	30
17	50	2	0.4	200	3	10	30
18	60	2	0.4	200	3	10	30
19	10	3	0.4	200	3	10	30
20	20	3	0.4	200	3	10	30
21	30	3	0.4	200	3	10	30
22	40	3	0.4	200	3	10	30
23	50	3	0.4	200	3	10	30
24	60	3	0.4	200	3	10	30
25	10	4	0.4	200	3	10	30
26	20	4	0.4	200	3	10	30
27	30	4	0.4	200	3	10	30
28	40	4	0.4	200	3	10	30
29	50	4	0.4	200	3	10	30
30	60	4	0.4	200	3	10	30
31	10	5	0.4	200	3	10	30
32	20	5	0.4	200	3	10	30
33	30	5	0.4	200	3	10	30
34	40	5	0.4	200	3	10	30
35	50	5	0.4	200	3	10	30
36	60	5	0.4	200	3	10	30
37	10	1	0.4	200	7	100	30
38	20	1	0.4	200	7	100	30
39	30	1	0.4	200	7	100	30
40	40	1	0.4	200	7	100	30
41	50	1	0.4	200	7	100	30
42	60	1	0.4	200	7	100	30

43	10	1	0.6	200	7	100	30
44	20	1	0.6	200	7	100	30
45	30	1	0.6	200	7	100	30
46	40	1	0.6	200	7	100	30
47	50	1	0.6	200	7	100	30
48	60	1	0.6	200	7	100	30
49	10	1	0.8	200	7	100	30
50	20	1	0.8	200	7	100	30
51	30	1	0.8	200	7	100	30
52	40	1	0.8	200	7	100	30
53	50	1	0.8	200	7	100	30
54	60	1	0.8	200	7	100	30
55	10	1	1.0	200	7	100	30
56	20	1	1.0	200	7	100	30
57	30	1	1.0	200	7	100	30
58	40	1	1.0	200	7	100	30
59	50	1	1.0	200	7	100	30
60	60	1	1.0	200	7	100	30
61	10	1	0.2	50	7	100	30
62	20	1	0.2	50	7	100	30
63	30	1	0.2	50	7	100	30
64	40	1	0.2	50	7	100	30
65	50	1	0.2	50	7	100	30
66	60	1	0.2	50	7	100	30
67	10	1	0.2	100	7	100	30
68	20	1	0.2	100	7	100	30
69	30	1	0.2	100	7	100	30
70	40	1	0.2	100	7	100	30
71	50	1	0.2	100	7	100	30
72	60	1	0.2	100	7	100	30
73	10	1	0.2	150	7	100	30
74	20	1	0.2	150	7	100	30
75	30	1	0.2	150	7	100	30
76	40	1	0.2	150	7	100	30
77	50	1	0.2	150	7	100	30
78	60	1	0.2	150	7	100	30
79	10	1	0.2	250	7	100	30
80	20	1	0.2	250	7	100	30
81	30	1	0.2	250	7	100	30
82	40	1	0.2	250	7	100	30
83	50	1	0.2	250	7	100	30
84	60	1	0.2	250	7	100	30
85	10	1	0.2	200	3	100	30
86	20	1	0.2	200	3	100	30
87	30	1	0.2	200	3	100	30
88	40	1	0.2	200	3	100	30
89	50	1	0.2	200	3	100	30
90	60	1	0.2	200	3	100	30

91	10	1	0.2	200	5	100	30
92	20	1	0.2	200	5	100	30
93	30	1	0.2	200	5	100	30
94	40	1	0.2	200	5	100	30
95	50	1	0.2	200	5	100	30
96	60	1	0.2	200	5	100	30
97	10	1	0.2	200	9	100	30
98	20	1	0.2	200	9	100	30
99	30	1	0.2	200	9	100	30
100	40	1	0.2	200	9	100	30
101	50	1	0.2	200	9	100	30
102	60	1	0.2	200	9	100	30
103	10	1	0.2	200	11	100	30
104	20	1	0.2	200	11	100	30
105	30	1	0.2	200	11	100	30
106	40	1	0.2	200	11	100	30
107	50	1	0.2	200	11	100	30
108	60	1	0.2	200	11	100	30
109	10	1	0.2	200	7	20	30
110	20	1	0.2	200	7	20	30
111	30	1	0.2	200	7	20	30
112	40	1	0.2	200	7	20	30
113	50	1	0.2	200	7	20	30
114	60	1	0.2	200	7	20	30
115	10	1	0.2	200	7	40	30
116	20	1	0.2	200	7	40	30
117	30	1	0.2	200	7	40	30
118	40	1	0.2	200	7	40	30
119	50	1	0.2	200	7	40	30
120	60	1	0.2	200	7	40	30
121	10	1	0.2	200	7	60	30
122	20	1	0.2	200	7	60	30
123	30	1	0.2	200	7	60	30
124	40	1	0.2	200	7	60	30
125	50	1	0.2	200	7	60	30
126	60	1	0.2	200	7	60	30
127	10	1	0.2	200	7	80	30
128	20	1	0.2	200	7	80	30
129	30	1	0.2	200	7	80	30
130	40	1	0.2	200	7	80	30
131	50	1	0.2	200	7	80	30
132	60	1	0.2	200	7	80	30
133	10	1	0.2	200	7	100	20
134	20	1	0.2	200	7	100	20
135	30	1	0.2	200	7	100	20
136	40	1	0.2	200	7	100	20
137	50	1	0.2	200	7	100	20
138	60	1	0.2	200	7	100	20

139	10	1	0.2	200	7	100	10
140	20	1	0.2	200	7	100	10
141	30	1	0.2	200	7	100	10
142	40	1	0.2	200	7	100	10
143	50	1	0.2	200	7	100	10
144	60	1	0.2	200	7	100	10
145	10	1	0.2	200	7	100	5
146	20	1	0.2	200	7	100	5
147	30	1	0.2	200	7	100	5
148	40	1	0.2	200	7	100	5
149	50	1	0.2	200	7	100	5
150	60	1	0.2	200	7	100	5

FR_1: Flow rate of electrolyte, FR_2: Flow rate of oxygen, [KOH]: Concentration of electrolyte, [MO]: Concentration of methyl orange, Temp: Temperature, T: Time, V: Volt.

Table 8.2 The experimental results of the performance of electrochemical process for methyl orange oxidation in TBER at 60 min.

Run	Volt (V)	Conc. Of KOH (M)	Flow rate of KOH (ml/min)	Flow rate of O_2 (L/min)	Cmo_o (ppm)	Cmo (ppm)	Temp. °C.	Removal %
1	0.5	0.4	200	3	10	4.15	30	58.4
2	1	0.4	200	3	10	1,95	30	80.4
3	2	0.4	200	3	10	2.46	30	75.3
4	3	0.4	200	3	10	2.9	30	70.9
5	4	0.4	200	3	10	3.36	30	66.3
6	5	0.4	200	3	10	3.73	30	62.62
7	1	0.2	200	7	100	34.9	30	65.09
8	1	0.4	200	7	100	40.05	30	59.9
9	1	0.6	200	7	100	47.5	30	52.4
10	1	0.8	200	7	100	52.9	30	47.0
11	1	1.0	200	7	100	60.22	30	39.7
12	1	0.2	50	7	100	41.2	30	58.7
13	1	0.2	100	7	100	36.8	30	63.1
14	1	0.2	150	7	100	30.77	30	69.2
15	1	0.2	200	7	100	21.1	30	78.8
16	1	0.2	250	7	100	27.38	30	72.6
17	1	0.2	200	3	100	45.62	30	54.3
18	1	0.2	200	5	100	39.15	30	60.8
19	1	0.2	200	7	100	21.11	30	78.8
20	1	0.2	200	9	100	28.14	30	71.8
21	1	0.2	200	11	100	33.98	30	66.0
22	1	0.2	200	7	20	3.06	30	96.9
23	1	0.2	200	7	40	6.98	30	93.0
24	1	0.2	200	7	60	10.85	30	89.1
25	1	0.2	200	7	80	15.9	30	84.0
26	1	0.2	200	7	100	21.1	30	78.8
27	1	0.2	200	7	100	45.73	5	54.2
28	1	0.2	200	7	100	40.48	10	59.5
29	1	0.2	200	7	100	30.04	20	69.9
30	1	0.2	200	7	100	21.1	30	78.8

Table 8.3 Results of the kinetic studies (100 ppm, 1 V, 0.2 M KOH, 200 mL/min KOH, 7 L/min O_2.

Run	Temp (°C)	Cmo_o (ppm)	Time (min)	$Ln(Cmo_o/Cmo)$	Cmo (ppm)	Removal %	Run	Temp (°C)	Cmo_o (ppm)	Time (min)	$Ln(Cmo_o/Cmo)$	Cmo (ppm)	Removal %
1	5	100	10	0.24	78.81	21.18	13	20	100	10	0.48	62.05	37.94
2	5	100	20	0.36	69.86	30.13	14	20	100	20	0.61	54.33	45.66
3	5	100	30	0.47	62.59	37.40	15	20	100	30	0.75	47.19	52.80
4	5	100	40	0.58	56.04	43.95	16	20	100	40	0.91	40.23	59.76
5	5	100	50	0.71	49.25	50.74	17	20	100	50	1.09	33.64	66.35
6	5	100	60	0.78	45.73	54.26	18	20	100	60	1.20	30.04	69.95
7	10	100	10	0.34	70.83	29.16	19	30	100	10	0.68	50.68	49.31
8	10	100	20	0.46	63.40	36.59	20	30	100	20	0.84	43.10	56.89
9	10	100	30	0.57	56.31	43.68	21	30	100	30	1.04	35.39	64.60
10	10	100	40	0.71	49.04	50.95	22	30	100	40	1.23	29.12	70.87
11	10	100	50	0.83	43.75	56.24	23	30	100	50	1.41	24.52	75.47
12	10	100	60	0.90	40.48	59.51	24	30	100	60	1.56	21.11	78.88

Table 8.4 Comparative removal by adsorption and in situ oxidation by H_2O_2 at operating conditions of 1 V, 0.2 M, 200 ml/min, 7 L/min, 100 ppm, and 30°C.

Time (min)	Adsorption		Electrochemical oxidation without O_2		Electrochemical oxidation by H_2O_2 with O_2	
	C_{mo}	Removal %	C_{mo}	Removal %	C_{mo}	Removal %
10	94.84	5.1	88.5	11.4	50.68	49.3
20	93.64	6.3	85.56	14.4	43.10	56.8
30	92.78	7.2	80.58	19.4	35.39	64.6
40	91.7	8.2	76.42	23.5	29.12	70.8
50	91.01	8.9	74.33	25.6	24.52	75.4
60	90.39	9.6	72.88	27.1	21.11	78.8

Table 8.5 Thermodynamic parameters for adsorption of MO on CB-PTFE

Temperature (K)	K_C	$\Delta G°$ (kj/mol)	$\Delta H°$ (kj/mol)	$\Delta S°$ (kj/molK)
278.15	1.187	-0.395	31.867	0.116
283.15	1.471	-0.907		
293.15	2.329	-2.061		
303.15	3.737	-3.322		